

# FINAL REPORT

**Project Title:** Advanced Variance Reduction for Global  $k$ -Eigenvalue Simulations in MCNP

**Award Number:** DE-FG07-04ID14608

**Covering Period:** September 13, 2004 through September 12, 2007

**Date of Report:** May 16, 2008

**Recipient:** University of Michigan  
Department of Nuclear Engineering and Radiological Sciences  
Cooley Building, North Campus  
Ann Arbor, MI 48109-2104

**Subcontractors:** None

**Other Partners:** None

**Contacts:** Edward W. Larsen (PI)  
(734) 936-0124  
edlarsen@umich.edu

William R. Martin (co-PI)  
(734) 764-5534  
wrm@umich.edu

**Project Team:**

DOE-HQ contact: Nancy Elizondo, elizonna@id.doe.gov  
Contract specialist: Kate Koorhan, kkoorhan@umich.edu  
Accountant: Shannon Thomas, noonie@umich.edu

**Project Objectives:**

- Develop advanced variance reduction techniques, based on the Variational Variance Reduction (VVR) methodology, for improving the efficiency of global reactor calculations, and incorporate these results into the production Monte Carlo code (MCNP5).
- Implement this new version of MCNP5 on a Linux cluster at the University of Michigan, in order to process these histories faster than presently possible on a typical workstation.
- Test this methodology for realistic problems.

## **Background:**

The estimation of  $k$ -eigenvalues and eigenfunctions for practical reactor and other nuclear configurations is an essential computational problem in nuclear engineering. Present-day computer codes for simulating  $k$ -eigenvalue problems are either purely deterministic or purely stochastic (Monte Carlo). Deterministic methods employ a discretization of all the independent variables in the Boltzmann equation: space, direction of flight, and energy. This discretization replaces the continuous Boltzmann equation by a (typically) large linear algebraic system of equations, which is then solved. This approach introduces truncation errors in each of the independent variables and is limited by the shape and size of the grids used for each independent variable. Alternatively, the stochastic or Monte Carlo method (i) uses pseudo-random number sequences to simulate the random histories of individual neutrons, and (ii) averages the results over many histories.

Of the two approaches, Monte Carlo is often considered to be more accurate because it requires no angular or energy discretization, and in principle it can handle arbitrary geometries. However, Monte Carlo solutions have statistical errors that decrease slowly with the number of histories, i.e. with the computing time. Also, if nonanalog Monte Carlo methods are used, which is often the case, then significant user time can be required to develop – through a potentially lengthy trial-and-error process – adequate biasing parameters. Thus, while Monte Carlo solutions can be more accurate, they are often much more expensive for the user to set up and run.

The goal of this project has been to (i) combine concepts from deterministic and stochastic methods to obtain an improved *hybrid* strategy for obtaining Monte Carlo estimates of  $k$ -eigenvalues and their corresponding eigenfunctions, and (ii) implement these methods in MCNP5. This work complements previous recent work in which deterministic and Monte Carlo methods have been merged to enhance the solution of Monte Carlo source-detector problems [1,2].

In all the hybrid methods that we have investigated for both fixed-source and eigenvalue problems, we have preserved the unbiased nature of Monte Carlo simulations. The deterministic elements of our work are designed to (i) increase the efficiency (and reduce the variance) of the Monte Carlo simulations; and (ii) retain the principle that, as the number of particle histories tends to infinity, the Monte Carlo estimate should become exact. For this project, the goal of our work is to develop and implement a new hybrid method that will perform difficult  $k$ -eigenvalue calculations more accurately and efficiently, and with less user input.

## **Summary of Work Done for This Project:**

In work done prior to this project, we explored the use of a variational functional to estimate the criticality  $k$  of a fissile system [3,4]. The variational functional is more accurate than the conventional functional used in Monte Carlo  $k$ -calculations, but it depends on accurate estimates of both the forward and adjoint eigenfunctions. (The less-accurate conventional functional depends

only on an accurate estimate of the forward eigenfunction.) In this preliminary work, we showed that one can estimate the adjoint eigenfunction either by an initial deterministic calculation or by Monte Carlo, and we estimated the forward eigenfunction by Monte Carlo. We then discovered that the Monte Carlo estimation of forward and adjoint eigenfunctions is enhanced by a new *correcton* procedure in which Monte Carlo is used *not* to directly estimate the eigenfunction, but rather to estimate the *multiplicative correction* to an inexpensive deterministic estimate of the eigenfunction [5,6,7]. (For example, this deterministic estimate could be obtained from a diffusion calculation.)

Because (i) the variational functional is more accurate than the conventional functional and (ii) the correcton procedure yielded more accurate estimates of the flux for fixed-source problems, we reasoned that for both reasons, this procedure should yield more accurate estimates of the eigenfunction and eigenvalue for eigenvalue problems. The down side is that (i) the variational functional for  $k$  requires estimations of both the forward and adjoint eigenfunctions (current methods for estimating eigenvalues use a simpler but less accurate functional that only requires an estimate of the forward eigenfunction) and (ii) evaluating the variational functional requires more computer algebra, and hence more time and expense. In our early work, the plusses greatly outweighed the minuses, giving a significantly more efficient hybrid method.

Based on this experience, we originally proposed for this project to numerically estimate  $k$ -eigenvalues by (i) using the more accurate variational functional [3,4], and (ii) determining the forward and adjoint eigenfunctions using the more accurate correcton procedure.

During the first year of the project, we developed and tested the originally-proposed correcton procedure for estimating a forward (or adjoint) eigenfunction [5,6,7]. This approach was quite successful for reactor shielding problems, and for such applications was written up and published in *Nuclear Science and Engineering* [7]. Unfortunately, we discovered that the correcton method does not overcome a deficiency that plagues all known Monte Carlo  $k$ -eigenvalue simulations: the unreliable estimate of the eigenfunction for “difficult” optically thick problems. This deficiency manifests itself in slightly different ways for two different types of problems:

- For optically thick fissile systems (such as a commercial nuclear reactor core), it is difficult for neutrons on one side of the system to communicate with distant parts of the system. For this reason, an unphysical “tilting” or “undersampling” of the Monte Carlo estimate of the eigenfunction occurs, except when an extraordinarily large number of Monte Carlo particles per generation is used. The manifestation of this effect is that instead of acquiring a classic symmetric “cosine” shape, the eigenfunction tilts and slowly – from one generation to the next – wobbles in random and asymmetric ways around the basic cosine shape. When viewed over a sequence of many generations, this wobbling is suggestive of a flag blowing in the wind.
- For optically thick systems containing numerous small but weakly-coupled fissile regions (such as spent nuclear fuel storage containers), it is difficult for neutrons in one fissile region to communicate with the other fissile regions. In this case, Monte Carlo estimates of the

eigenfunction tend to have the correct *shapes* within each fissile region, but the *amplitude* of the eigenfunction estimates – which depends very sensitively on the few neutrons that propagate between fissile regions – is incorrect. These relative amplitudes change slowly and randomly from one fission generation to the next. As the fissile systems become increasingly isolated, the problem for estimating the  $k$ -eigenfunction becomes more difficult – the problem becomes increasingly ill-posed. (In contrast, the single thick fissile regions discussed in the first bullet above do not become ill-posed as the system becomes thick.)

The only known remedy for these deficiencies – using a sufficient number of Monte Carlo particles per generation – is impractical, due to the potentially huge number of Monte Carlo particles required.

During much of the first and second years of the project, we struggled to overcome these difficulties, along with the inherent disadvantage that the variational approach requires separate eigenfunction simulations for the forward and adjoint eigenfunctions.

Late in the second year of the project we devised a new *Functional Monte Carlo (FMC)* method that showed significant promise to overcome these difficulties. The FMC method differs significantly from the standard and the proposed correction/variational Monte Carlo methods, in which Monte Carlo estimates of the eigenfunction are obtained and are introduced into functionals to determine the eigenvalue  $k$ . In particular, *the FMC method does not directly require accurate Monte Carlo estimates of the eigenfunction*. Instead, the FMC method requires accurate estimates of local nonlinear *functionals*, which are much less sensitive to statistical errors than estimates of the eigenfunction itself.

A basic sketch of the FMC method for monoenergetic planar-geometry problems is described as follows.

1. One begins with the continuous eigenvalue problem, stated in terms of the Boltzmann equation for the eigenfunction  $\psi(x, \mu)$  and the eigenvalue  $k$ . The equations that define the FMC method are derived directly from the Boltzmann equation, with no error.
2. One introduces a spatial grid defined by points  $x_{j+1/2}$  (for 1-D geometry). This grid is used to calculate space-angle moments of the solution, but these various moments will have no truncation errors.
3. One defines functions  $f_{j+1/2}(x)$  and  $g_{j+1/2}(x)$  which are *local* to  $x_{j+1/2}$ , i.e. which are nonzero only on the interval  $x_{j-1/2} < x < x_{j+3/2}$ .
4. One operates on the Boltzmann equation by the operator:

$$L_{j+1/2}^n = \int_{x_{j-3/2}}^{x_{j+3/2}} \int_{-1}^1 \mu^n f_{j+1/2}(x)(\cdot) d\mu dx$$

for  $n = 0$  and 1 and suitable choices of  $f_{j+1/2}(x)$ , to obtain an exact system of equations for the space-angle moments of  $\psi$ :

$$\phi_{j+1/2}^n = \int_{x_{j-3/2}}^{x_{j+3/2}} \int_{-1}^1 \mu^n f_{j+1/2}(x) \psi(x, \mu) d\mu dx .$$

5. The odd- $n$  moments  $\phi_{j+1/2}^1$  are eliminated in terms of the even- $n$  moments  $\phi_{j+1/2}^0$  and  $\phi_{j+1/2}^2$ .
6. One multiplies and divides various terms in the resulting equations by

$$\Phi_{j+1/2} = \int_{x_{j-3/2}}^{x_{j+3/2}} \int_{-1}^1 g_{j+1/2}(x) \psi(x, \mu) d\mu dx \quad (1)$$

to obtain a discrete system of equations for  $\Phi_{j+1/2}$  and  $k$ , containing nonlinear *functionals* of the following form:

$$F_{j+1/2}^n = \frac{\int_{x_{j-3/2}}^{x_{j+3/2}} \int_{-1}^1 \mu^n f_{j+1/2}(x) \psi(x, \mu) d\mu dx}{\int_{x_{j-3/2}}^{x_{j+3/2}} \int_{-1}^1 g_{j+1/2}(x) \psi(x, \mu) d\mu dx} . \quad (2)$$

7. The above process of constructing equations for  $\Phi_{j+1/2}$  and  $k$  introduces no errors. Therefore, if the functionals  $F_{j+1/2}^n$  are known exactly, then the resulting algebraic system of equations determine  $\Phi_{j+1/2}$  and  $k$  *exactly*.
8. In the FMC method, (i) Monte Carlo is used to estimate functionals of the form defined by Eq. (1), and then (ii) the resulting discrete system of equations is solved for  $\Phi_{j+1/2}$  and  $k$ . Because the functionals contain statistical errors and the equations for  $\Phi_{j+1/2}$  contain no truncation errors, the resulting estimates of  $\Phi_{j+1/2}$  contain only statistical errors. As the statistical errors in the functionals become small, the subsequent statistical errors in  $\Phi_{j+1/2}$  will also become small.

Thus, as stated above, the FMC method does not require that accurate estimates of the eigenfunction  $\psi(x, \mu)$  be obtained. Instead, the method requires that accurate estimates of *functionals* of the form defined in Eq. (2) be obtained. This is a much easier task because these functionals, being nonlinear and local and containing only low-order angular moments of  $\psi$ , are much less sensitive to statistical fluctuations than direct estimates of the eigenfunction  $\psi$ .

The remaining question is: are the discrete equations for  $\Phi_{j+1/2}$  [see Eq. (1)] and  $k$  sufficiently insensitive to statistical errors in the functionals  $F_{j+1/2}^n$ ? In other words, do small statistical errors in the functionals  $F_{j+1/2}^n$  lead to sufficiently small statistical errors in  $\Phi_{j+1/2}$  and  $k$ ? If the answer is yes, and if Monte Carlo estimates of  $F_{j+1/2}^n$  indeed have small statistical errors, then the final statistical errors in the estimate of the eigenfunction and  $k$  will be small – potentially much smaller than standard Monte Carlo estimates.

During the third year of the project, we implemented and tested the FMC method for planar geometry one-group and multigroup problems. The extension of the FMC method to 3-D geometries and general energy-dependent problems is relatively straightforward, but there was little time left in the project and it seemed logical to begin by testing the method in 1-D. Our numerical experiments have shown the following:

1. For optically thick fissile systems, such as commercial reactor cores, the FMC method yields estimates of the eigenfunction and  $k$  that are *much* more accurate than the estimates obtained by standard Monte Carlo. For the problems that we have run, we see increases of the Figure of Merit for estimates of  $k$  of between one and three orders of magnitude.
2. For optically thick systems containing *isolated* fissile regions, such as nuclear waste storage tanks, the FMC method yields accurate estimates of the eigenvalue, but not necessarily the eigenfunction. The reason for the relatively inaccurate estimate of the eigenfunction is that for problems of this type, the eigenfunction can be extremely sensitive to very small changes in the system, and hence the problems can be poorly-posed for the eigenfunction.

To explain this last assertion, if two identical fissile spheres are separated and surrounded by an infinite absorbing region, the  $k$ -eigenfunction for this infinite system will be symmetric about the plane that symmetrically separates the two spheres. If the distance between the two spheres is large, so that it is rare for neutrons in one sphere to propagate to the other, then a very small change in the value of  $\nu\Sigma_f$  in one sphere will have (i) a major change in the eigenfunction (which will no longer be symmetric but become significantly peaked around the more fissile sphere), but (ii) only a small change on the eigenvalue  $k$ . Therefore, problems of this nature will have eigenfunctions that can be *very* sensitive to small changes in the physical data, but eigenvalues that will be much less sensitive.

In the FMC method, the small statistical fluctuations in the functionals can be viewed as corresponding to small statistical fluctuations in the underlying problem data. These small fluctuations in the functionals can yield large changes in the estimates of the eigenfunction, but only small changes in the estimate of  $k$ .

This reasoning indicates that *any* numerical method to estimate  $k$  for these kinds of systems will at best be able to confidently estimate an accurate  $k$ . The problems are inherently ill-posed for the eigenfunction. Any approximation in the calculation could lead to a major error in the estimate of the eigenfunction. (Fortunately, for these problems, estimates of the eigenvalue are usually much more useful than estimates of the eigenfunction.)

3. A well-known difficulty in standard Monte Carlo estimates of  $k$  is that the estimated variance in  $k$  can be significantly smaller than the true variance. This can cause the user to erroneously believe that the calculation yields significantly more accurate estimates than it actually does. This underestimation of the variance is caused by strong correlations between the estimates

of the fission source in successive fission generations. In our simulations of  $k$  using the FMC method, these strong correlations in the fission source are *much* smaller, so it seems likely that the FMC estimates of the variance are much closer to the true variance than the standard estimates. However, we have not been able to investigate this fully.

The current status of this work is described below. (Some of this work was done after the official conclusion of the project in September, 2007.)

- The FMC method generalizes to multigroup problems without significant difficulty. We have extended our theory and code to these problems and have performed numerous numerical simulations. The basic advantages of the FMC method observed for one energy group extend with little variation to multiple energy groups.
- We have not yet been able to extend the method to 1-D continuous-energy problems, or to energy-dependent problems with anisotropic scattering. The inclusion of continuous energy and anisotropic scattering yields extra terms in the discrete equations that are not as straightforward to treat as in the case of isotropic scattering, and it is not clear how to optimally treat them. This should not be a major hurdle, but it will require time to overcome.
- We also have not been able to extend our work to multi-D. Doing this should not be conceptually difficult, but will require time.
- We were not able to implement the FMC method in MCNP-5. Unfortunately, this aspect of our original proposal remains unfulfilled.
- We presented our 1-D monoenergetic results at the winter 2007 ANS conference [8]. The organizers of this conference were sufficiently impressed with these results that they invited us to expand the abstract to a journal article and submit it to *Nuclear Science and Engineering* (NS&E), where it was quickly reviewed, and after minor revisions, accepted for publication. It is scheduled to be published in June, 2008 [9]. The ANS abstract and NS&E preprint are copied in appendices to this report.
- The FMC method described above yields very accurate estimates of the eigenfunction for optically thick systems. In this sense, the FMC method is *global*; it inherently yields accurate estimates of the flux everywhere in the system. With very little effort, the FMC method can be adapted to fixed source problems, where it could be used (for example) to generate global solutions for deep penetration shielding calculations. For these problems, some special techniques would have to be used to ensure that a sufficient number of Monte Carlo particles exist in the “deep” regions of the system so that accurate estimates of the functional are obtained in these regions. However, this is not a difficult task.
- Currently, we are seeking funding to continue this work, either for eigenvalue or fixed-source problems. We continue to believe that the concept of the FMC method has significant promise.

## Budget Data:

Note: The “actual spending” reflects the money actually spent on the project in the corresponding periods.

Phase/Budget Period			Approved Spending Plan			Actual Spending		
			DOE Amount	Cost Share	Total	DOE Amount	Cost Share	Total
	From	To						
Year 1	10/04	9/05	97,585	-	97,585	93,968	-	93,968
Year 2	10/05	9/06	99,974	-	99,974	154,327	-	154,327
Year 3	10/06	9/07	102,424	-	102,424	50,772	-	50,772
Totals:			299,983	-	299,983	299,067	-	299,067

## References:

1. A. Haghghat and J.C. Wagner, “Monte Carlo Variance Reduction with Deterministic Importance Functions,” *Prog. Nucl. Energy* **42**, 25 (2003).
2. H.P. Smith and J.C. Wagner, “A Case Study in Manual and Automated Monte Carlo Variance Reduction with a Deep Penetration Reactor Shielding Problem,” *Nucl. Sci. Eng.* **149**, 23 (2005).
3. J.D. Densmore and E.W. Larsen, “Variational Variance Reduction for Particle Transport Eigenvalue Calculations Using Monte Carlo Adjoint Simulation,” *J. Comp. Phys.* **192**, 387 (2003).
4. J.D. Densmore and E.W. Larsen, “Variational Variance Reduction for Monte Carlo Eigenvalue and Eigenfunction Problems,” *Nucl. Sci. Eng.* **146**, 121 (2004).
5. A.B. Wollaber and E.W. Larsen, “A Hybrid Monte Carlo-Deterministic Method for Global Transport Calculations,” Proc. ANS Topical Meeting: M&C 2005, International Topical Meeting on Mathematics and Computation, Supercomputing, Reactor Physics and Nuclear and Biological Applications, Sept. 12-15, 2005, Avignon, France (2005).
6. T.L. Becker and E.W. Larsen, Multigroup Formulation of the Corrected Hybrid Monte Carlo / Deterministic Transport Method,” *Trans. Am. Nucl. Soc.* **95**, 550 (2006).
7. T.L. Becker, A.B. Wollaber, and E.W. Larsen, “A Hybrid Monte Carlo-Deterministic Method for Global Particle Transport Calculations,” *Nucl. Sci. Eng.* **155**, 155 (2007).
8. E.W. Larsen and J. Yang, “New ‘Monte Carlo Functional’ Methods for Estimating  $k$ -Eigenvalues and Eigenfunctions,” *Trans. Am. Nucl. Soc.* **97**, 469 (2007).
9. E.W. Larsen and J. Yang, “A Functional Monte Carlo Method for  $k$ -Eigenvalue Problems,” *Nucl. Sci. Eng.* **159**, 1 (2008). (Scheduled to be published in the June 2008 issue.)



## Appendix:

In the following appendix, we include two publications that detail some of the accomplishments of the project. The first publication is a recent 3-page American Nuclear Society conference abstract:

- “New ‘Monte Carlo Functional’ Methods for Estimating  $k$ -Eigenvalues and Eigenfunctions,” *Trans. Am. Nucl. Soc.* **97**, 469 (2007).

The second is a to-be-published 20-page article in *Nuclear Science and Engineering*:

- E.W. Larsen and J. Yang, “A Functional Monte Carlo Method for  $k$ -Eigenvalue Problems,” *Nucl. Sci. Eng.* **159**, 1 (2008). (Scheduled to be published in June, 2008.)

New “Monte Carlo Functional” Methods for Estimating  $k$ -Eigenvalues and Eigenfunctions

Edward W. Larsen, Jinan Yang

Department of Nuclear Engineering & Radiological Sciences, University of Michigan, Ann Arbor, MI, 48109  
 edlarsen@umich.edu, jinan@umich.edu

## INTRODUCTION

Monte Carlo methods for estimating  $k$ -eigenvalues and eigenfunctions can be problematic for optically thick fissile systems. In such problems, Monte Carlo estimates of the eigenfunctions often exhibit an unphysical “tilting,” caused by (i) a large dominance ratio, and (ii) the arbitrary amplitude of the eigenfunction and the inability of neutrons in one part of the system to “see” the amplitude of the solution in distant parts. In this abstract, we propose several new Monte Carlo methods that show a strong potential for remedying this difficulty. These methods solve the “high-order” Boltzmann equation by combining it with “low-order” equations obtained by taking space-angle moments of the high-order equation. The low-order equations contain nonlinear functionals of the solution of the high-order equation; these functionals make the high-order and low-order equations consistent. The procedure used here is based on the Quasidiffusion (QD) method for  $S_N$  problems [1]-[3], but the QD method differs because it uses only angular moments of the transport equation.

## DESCRIPTION OF THE METHODS

We consider for simplicity a planar-geometry, one-group  $k$ -eigenvalue problem with vacuum boundaries:

$$\mu \frac{\partial \psi}{\partial x}(x, \mu) + \Sigma_t(x)\psi(x, \mu) - \frac{\Sigma_s(x)}{2} \int_{-1}^1 \psi(x, \mu') d\mu'$$

$$= \frac{\nu \Sigma_f(x)}{2k} \int_{-1}^1 \psi(x, \mu') d\mu', \quad 0 < x < X, \quad (1a)$$

$$\psi(0, \mu) = 0, \quad 0 < \mu \leq 1, \quad (1b)$$

$$\psi(X, \mu) = 0, \quad -1 \leq \mu < 0. \quad (1c)$$

To begin, we follow the QD procedure and operate on Eq. (1) by  $\int_{-1}^1 \mu^n(\cdot) d\mu$  for  $n = 1$  and 2. Defining  $\phi_n(x) = \int_{-1}^1 \mu^n \psi(x, \mu) d\mu$ , we get:

$$\frac{d\phi_1}{dx}(x) + \left( \Sigma_a(x) - \frac{\nu \Sigma_f(x)}{k} \right) \phi_0(x) = 0, \quad (2a)$$

$$\frac{d\phi_2}{dx}(x) + \Sigma_t(x)\phi_1(x) = 0. \quad (2b)$$

Solving Eq. (2b) for  $\phi_1(x)$  and introducing the result into Eq. (2a), we obtain:

$$-\frac{d}{dx} \frac{1}{\Sigma_t(x)} \frac{d\phi_2}{dx}(x) + \left( \Sigma_a(x) - \frac{\nu \Sigma_f(x)}{k} \right) \phi_0(x) = 0, \quad 0 < x < X. \quad (3)$$

Also, operating on Eq. (1b) by  $\int_0^1 2\mu(\cdot) d\mu$ , we get:

$$0 = \int_0^1 2\mu\psi(0, \mu) d\mu = \phi_1(0) + \int_{-1}^1 |\mu|\psi(0, \mu) d\mu. \quad (4)$$

Using Eq. (2b) to eliminate  $\phi_1(0)$ , we obtain:

$$0 = -\frac{1}{\Sigma_t(0)} \frac{d\phi_2}{dx}(0) + \int_{-1}^1 |\mu|\psi(0, \mu) d\mu. \quad (5)$$

A similar equation holds at  $x = X$ , which we will not write here. Eqs. (3) and (5) are exactly satisfied by the solution  $\psi$  of Eqs. (1).

Now we depart from the QD approach and take certain spatial moments of Eq. (3). To simplify the algebra, we assume that the system is homogeneous and impose a uniform grid on the system with  $J$  cells, each of width  $h = X/J$ . (However, this analysis can easily be extended to inhomogeneous media and nonuniform grids.) We define  $x_{j+1/2} = jh$  for  $0 \leq j \leq J$  to be the grid points;  $x_{j\pm 1/2}$  are the edges of the  $j^{\text{th}}$  cell. For  $0 \leq j \leq J$  we define the “tent” functions:

$$f_{1/2} = \begin{cases} \frac{1}{h}(x_{3/2} - x) & , \quad 0 < x < x_{3/2} \\ 0 & , \quad \text{otherwise} \end{cases}, \quad (6a)$$

$$f_{J+1/2} = \begin{cases} \frac{1}{h}(x - x_{J-1/2}) & , \quad x_{J-1/2} < x < X \\ 0 & , \quad \text{otherwise} \end{cases}, \quad (6b)$$

and for  $1 \leq j \leq J - 1$ ,

$$f_{j+1/2} = \begin{cases} \frac{1}{h}(x - x_{j-1/2}) & , \quad x_{j-1/2} < x < x_{j+1/2} \\ \frac{1}{h}(x_{j+3/2} - x) & , \quad x_{j+1/2} < x < x_{j+3/2} \\ 0 & , \quad \text{otherwise} \end{cases}. \quad (6c)$$

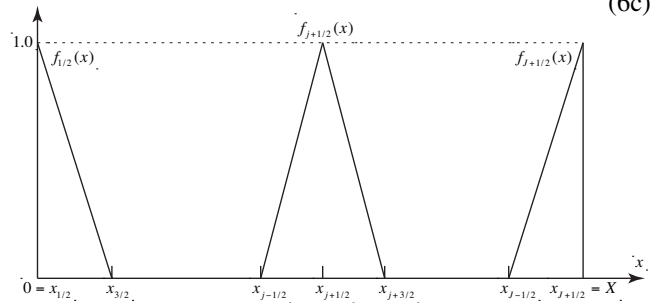


Figure 1: The Tent Functions

Now for  $1 \leq j \leq J - 1$ , we multiply Eq. (3) by  $f_{j+1/2}(x)$  and integrate over  $x_{j-1/2} < x < x_{j+3/2}$ . Carefully integrating by parts to unfold the derivatives of  $\phi_2(x)$ ,

we obtain:

$$-\frac{1}{\Sigma_t h} [\phi_2(x_{j+3/2}) - 2\phi_2(x_{j+1/2}) + \phi_2(x_{j-1/2})] + \left( \Sigma_a - \frac{\nu \Sigma_f}{k} \right) \int_{x_{j-1/2}}^{x_{j+3/2}} f_{j+1/2}(x) \phi_0(x) dx = 0 . \quad (7a)$$

Also, we multiply Eq. (3) by  $f_{1/2}(x)$  and integrate over  $0 < x < x_{1/2}$ . Carefully integrating by parts to unfold the derivatives of  $\phi_2$  and using Eq. (2b), we obtain:

$$-\phi_1(x_{1/2}) - \frac{1}{\Sigma_t h} [\phi_2(x_{3/2}) - \phi_2(x_{1/2})] + \left( \Sigma_a - \frac{\nu \Sigma_f}{k} \right) \int_{x_{1/2}}^{x_{3/2}} f_{1/2}(x) \phi_0(x) dx = 0 . \quad (7b)$$

A similar equation holds at  $x = X$ . Eqs. (7) are *exactly* satisfied by the solution  $\psi$  of Eqs. (1).

Now we define functions  $g_{j+1/2}(x)$  for  $0 \leq j \leq J$  which are “local” about  $x = x_{j+1/2}$ . In this paper, we consider two such sets of functions:

$$g_{j+1/2}(x) = \delta(x - x_{j+1/2}) , \quad (8a)$$

and

$$g_{j+1/2}(x) = \begin{cases} \frac{1}{h} & , \quad |x - x_{j+1/2}| < \frac{h}{2} \\ 0 & , \quad \text{otherwise} . \end{cases} \quad (8b)$$

(Other definitions of  $g_{j+1/2}$  are possible, including for example  $g_{j+1/2} = f_{j+1/2}$ .)

Defining:

$$\Phi_{j+1/2} = \int_0^X g_{j+1/2}(x) \phi_0(x) dx \quad (9)$$

and the nonlinear functionals:

$$E_{j+1/2} = \frac{\phi_2(x_{j+1/2})}{\int_0^X g_{j+1/2}(x) \phi_0(x) dx} , \quad (10a)$$

$$F_{j+1/2} = \frac{\frac{1}{h} \int_0^X f_{j+1/2}(x) \phi_0(x) dx}{\int_0^X g_{j+1/2}(x) \phi_0(x) dx} , \quad (10b)$$

$$B_{1/2} = \frac{\int_{-1}^1 2|\mu| \psi(0, \mu) d\mu}{\int_0^X g_{j+1/2}(x) \phi_0(x) dx} , \quad (10c)$$

we may rewrite Eqs. (7) as:

$$-\frac{1}{\Sigma_t h} (E_{j+3/2} \Phi_{j+3/2} - 2E_{j+1/2} \phi_{j+1/2} + E_{j-1/2} \phi_{j-1/2}) + \left( \Sigma_a - \frac{\nu \Sigma_f}{k} \right) h F_{j+1/2} \Phi_{j+1/2} = 0 , \quad 1 \leq j \leq J-1 , \quad (11a)$$

$$B_{1/2} \Phi_{1/2} - \frac{1}{\Sigma_t h} (E_{3/2} \Phi_{3/2} - E_{1/2} \Phi_{1/2}) + \left( \Sigma_a - \frac{\nu \Sigma_f}{k} \right) h F_{1/2} \Phi_{1/2} = 0 , \quad (11b)$$

with an equation similar to (11b) holding for  $j = J$ .

In this work, we use Eqs. (10) and (11) in the following way:

1. We run a standard Monte Carlo simulation of Eqs. (1), processing a suitable number of inactive cycles (generations) until the fission source is “converged,” and then processing a suitable number of active cycles. For each active cycle, we estimate  $k$ , and we obtain the standard Monte Carlo estimate of  $k$  by averaging the  $k$  for each cycle over all active cycles.
2. During each cycle, we also process the histories of the Monte Carlo particles to obtain estimates of the integrals used in Eqs. (10). At the end of each cycle, we calculate the functionals in Eqs. (10) using the estimated values of the integrals, and then we introduce these functionals into Eqs. (11) and solve the resulting system of discrete diffusion-like equations for  $k$  and  $\Phi_{j+1/2}$ . We average these estimates of  $k$  over all active cycles to obtain a new, and hopefully improved, estimate of the eigenvalue (and eigenfunction). The rationale behind this hope is that the functionals in Eqs. (10) are relatively insensitive to the amplitude of the Monte Carlo solution, and hence they should be more accurate than the direct Monte Carlo estimates of  $\psi$ . Thus, the solution of Eqs. (11) should be less sensitive to statistical error than the standard Monte Carlo estimates of  $\psi$  and  $k$ . This is the same rationale underlying the QD method. We call these methods “Monte Carlo Functional” (MCF) methods. We have tested two such methods, one with  $g_{j+1/2}$  defined by Eq. (8a), the other with  $g_{j+1/2}$  defined by Eq. (8b). For obvious reasons, we call the first method the “MCF Edge” method, and the second the “MCF Average” method.
3. We also considered an approximate method, in which rather than using Eq. (10b) to define  $F_{j+1/2}$ , we simply set  $F_{j+1/2} = 1$ . [In the system interior, this is the value given by Eq. (10b) when  $\phi_0(x)$  is a linear function of  $x$ .] Because Eqs. (11) reduce to low-order equations of the form of the QD equations, we call this the MCQD method.
4. In this work, the Monte Carlo particle histories are not affected by the low-order calculations of Eqs. (10) and (11). The standard Monte Carlo method for simulating particle histories is followed, but the results are processed as described above to obtain the new estimates of  $k$  and  $\Phi_{j+1/2}$ . A future method could use the results for  $\Phi_{j+1/2}$  to improve the actual Monte Carlo process for particle histories.
5. We emphasize that for the MCF methods, there is no truncation error; if the functionals in Eqs. (10) are

known exactly, then Eqs. (11) will yield the exact values of  $k$  and  $\Phi_{j+1/2}$ . Thus, although Eqs. (11) appear to be discretized, in fact there is no truncation error. (However, the MCQD method, which approximates  $F_{j+1/2}$ , does have a truncation error.)

**NUMERICAL RESULTS**

To test the methods described above, we considered a homogeneous slab with  $X = 200$  cm,  $\Sigma_\gamma = 0.084$  cm<sup>-1</sup>,  $\Sigma_f = 0.060$  cm<sup>-1</sup>,  $\Sigma_s = 0.856$  cm<sup>-1</sup>, and  $\nu = 2.4$ . We ran this (diffusive) problem with 50 inactive cycles and 200 active cycles, using 50,000 histories/cycle. The MCQD and MCF methods used a grid of  $h = 1.0$  cm = 1.0 mfp. The estimated values of  $k$ , with their estimated standard deviations, are given in Table 1 for the four Monte Carlo methods described above, and also for very finely-gridded diffusion and  $S_N$  calculations.

Method	Est. $k$	Est. St. Dev.
Diffusion	0.999435	na
$S_N$	0.999434	na
Analog MC	0.999009	0.000390
MCQD	0.999435	0.0000001
MCF Edge	0.999435	0.00000013
MCF Average	0.999435	0.00000011

Table 1: Estimated  $k$  and Standard Deviation

Also, the estimates of the eigenfunction for the  $S_N$  and Monte Carlo solutions are shown in Figure 2. [Note: the four Monte Carlo estimates of  $\Phi$  are averaged over the 200 active cycles.]

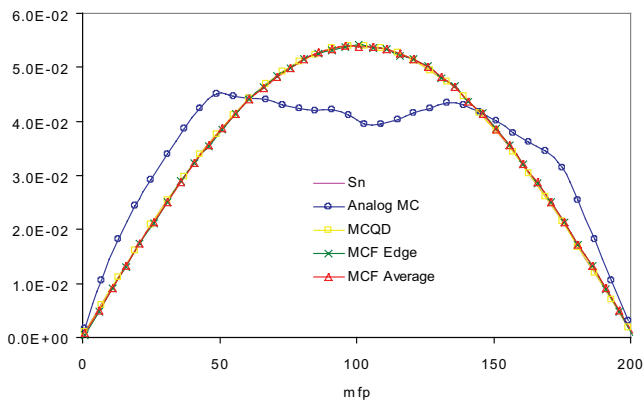


Figure 2: Estimates of the  $k$ -Eigenfunction

We see that the standard Monte Carlo estimate of  $\phi$  is significantly in error, and the error in the standard Monte Carlo estimate of  $k$  is much larger than the corresponding error in  $k$  for the MCQD and MCF methods. (The truncation error in the MCQD method is not apparent for this problem.) Also, the standard Monte Carlo estimate of  $k$  has

a much larger estimated standard deviation than the new estimates of  $k$ .

We comment that the MCQD and MCF estimates of the eigenfunction for each cycle appear to the eye to be almost as accurate as the average (over 100 active cycles) shown in Figure 2, while the standard Monte Carlo estimate of the eigenfunction for each cycles is much “noisier” than the plot shown in Figure 2.

These preliminary calculations show that using Monte Carlo simulations to estimate nonlinear functionals of the eigenfunction – which can be much more stable and accurate than estimates of the eigenfunction itself – can *indirectly* yield much more accurate estimates of the eigenfunction and eigenvalue.

**CONCLUSIONS**

We have presented new hybrid (MCQD and MCF) Monte Carlo methods for  $k$  eigenvalue/eigenfunction problems. The new methods differ from conventional Monte Carlo methods by the use of estimates of nonlinear functionals of the flux to indirectly obtain estimates of the eigenfunction and eigenvalue. (The MCQD method described here has truncation errors, but the two MCF methods do not.) For the problems tested, the nonlinear functionals are much more accurate than the direct Monte Carlo estimates of the eigenfunction; for this reason, the MCQD and MCF estimates of the eigenfunction and eigenvalue have much smaller variance than in standard Monte Carlo. In future work, we plan to extend the MCF method to realistic multi-D problems with anisotropic scattering and energy dependence.

**REFERENCES**

- [1] V.Ya. Gol’din, “A Quasi-Diffusion Method for Solving the Kinetic Equation,” *ZH. Vych. Mat.* **4**, 1078 (1964). English translation published in *USSR Comp. Math. and Math. Phys.* **4**, 6, 136 (1967).
- [2] D.Y. Anistratov and V.Ya. Gol’din, “Nonlinear Methods for Solving Particle Transport Problems,” *Transport Theory Stat. Phys.* **22**, 42 (1993).
- [3] D.Y. Anistratov, “Consistent Spatial Approximation of the Low-Order Quasidiffusion Equations on Coarse Grids,” *Nucl. Sci. Eng.* **149**, 138 (2005).

## A Functional Monte Carlo Method for $k$ -Eigenvalue Problems

Edward W. Larsen\* and Jinan Yang

University of Michigan  
Department of Nuclear Engineering and Radiological Sciences  
Ann Arbor, Michigan 48109-2104

Received November 6, 2007

Accepted January 17, 2008

**Abstract**—*In Monte Carlo simulations of  $k$ -eigenvalue problems for optically thick fissile systems with a high dominance ratio, the eigenfunction is often poorly estimated because of the undersampling of the fission source. Although undersampling can be addressed by sufficiently increasing the number of particles per cycle, this can be impractical in difficult problems. Here, we present a new functional Monte Carlo (FMC) method that minimizes this difficulty for many problems and yields a more accurate estimate of the  $k$ -eigenvalue. In the FMC method, standard Monte Carlo techniques do not directly estimate the eigenfunction; instead, they directly estimate certain nonlinear functionals that depend only weakly on the eigenfunction. The functionals are then used to more accurately estimate the  $k$ -eigenfunction and the eigenvalue. Like standard Monte Carlo methods, the FMC method has only statistical errors that limit to zero as the number of particles per cycle and the number of cycles become large. We provide numerical results that illustrate the advantages and limitations of the new method.*

### I. INTRODUCTION

Monte Carlo simulations of  $k$ -eigenvalue problems for optically thick fissile systems with high dominance ratios are often problematic because of a limited ability to accurately estimate the eigenfunction. This phenomenon has been called undersampling of the fission source. Undersampling can be addressed by sufficiently increasing the number of particles per cycle, but for difficult problems this can be prohibitively costly. A consequence of undersampling is that the fission source “wobbles” or “tilts” and fails to converge, even after many cycles. The problems associated with undersampling have been known for many years and have been examined in several recent publications.<sup>1–6</sup>

In this article we propose a new functional Monte Carlo (FMC) method for  $k$ -eigenvalue problems that helps to minimize the undesirable effects of undersampling. The FMC method does not employ standard Monte Carlo particle transport techniques to directly estimate the eigenfunction and the eigenvalue. Instead, the FMC method uses these techniques to directly estimate certain nonlinear functionals, which depend weakly on the eigen-

function. After these functionals are estimated, they are used to calculate the  $k$ -eigenfunction and the eigenvalue. Because the functionals depend weakly on the eigenfunction, the resulting estimates of the  $k$ -eigenfunction and the eigenvalue are generally more accurate and have less statistical noise than estimates obtained using conventional Monte Carlo methods. This is not the case in problems with loosely coupled fissile regions, where the FMC eigenfunction estimates have greater cycle-to-cycle statistical variation than in standard Monte Carlo. Nonetheless, even in these problems, the FMC estimate of the eigenvalue is experimentally seen to be more accurate.

The FMC method is related to the deterministic quasi-diffusion (QD) method,<sup>7–9</sup> sometimes called the variable Eddington factor method.<sup>10</sup> This iterative technique for eigenvalue (and fixed-source) problems does *not* employ high-order transport sweeps to directly estimate the eigenfunction but rather to directly estimate Eddington factors, which depend weakly on the eigenfunction. The Eddington factors are then used in a low-order quasi-diffusion eigenvalue problem to determine new estimates of the eigenvalue and the eigenfunction. These estimates are used to construct an updated fission source, which enables a new QD iteration to begin. Because the Eddington factors generally depend weakly on the

---

\*E-mail: edlarsen@umich.edu

eigenfunction, the QD iteration process usually converges rapidly.

The QD method is a deterministic approach for solving particle transport problems, and its converged estimates of the scalar flux have spatial and angular truncation errors. The QD method can be implemented with Monte Carlo–estimated Eddington factors<sup>11</sup>; the resulting scalar flux estimates have spatial truncation errors and statistical errors, due to the Monte Carlo–estimated Eddington factors.

Like the QD method, the FMC method employs a high-order particle transport process to estimate nonlinear functionals, which are then used in a low-order equation to estimate the eigenfunction and the eigenvalue. (One FMC functional is closely related to the QD Eddington factor.) Another similarity is that the QD and FMC eigenfunctions are estimated on a preassigned spatial grid.

The FMC method differs from the QD method in the following ways: (a) the FMC method uses Monte Carlo (rather than a deterministic method) to perform the high-order calculations used to estimate the functionals, (b) the FMC method is noniterative, and (c) the FMC method yields Monte Carlo estimates of the eigenfunction and the eigenvalue that have no spatial truncation errors. The only errors in the FMC estimates of the  $k$ -eigenfunction and the eigenvalue are due to the statistical errors in the Monte Carlo estimates of the functionals. In this sense, the FMC method is a pure Monte Carlo method—although the use of a spatial grid could tempt one to think otherwise.

In numerical testing, we have found that the FMC method significantly reduces the tilting that is often seen in simulations of systems containing one large fissile region, or in systems with tightly coupled fissile regions (e.g., nuclear reactor cores). For these problems, FMC estimates of the  $k$ -eigenfunctions and the eigenvalues are significantly more accurate than those obtained using standard Monte Carlo methods. Problems involving weakly coupled fissile regions (e.g., storage tanks for spent fuel rods) are inherently more difficult because the eigenfunctions for these problems can be highly sensitive to small perturbations. For such problems, the FMC estimates of the eigenfunction have larger variations from one cycle to the next than standard Monte Carlo estimates. Nonetheless, our numerical simulations indicate that the FMC estimate of the eigenvalue is more accurate than standard Monte Carlo estimates.

The remaining sections of this paper are organized as follows. In Sec. II we present the mathematical theory of the FMC method in the context of a monoenergetic planar geometry  $k$ -eigenvalue problem. (We have implemented the FMC method for planar geometry multi-group problems, and the FMC method can be extended to three-dimensions; however, these generalizations will not be discussed here.) In Sec. III we compare the FMC and standard Monte Carlo numerical simulations of  $k$ -eigenfunctions and the eigenvalues for three difficult problems. We conclude with a discussion in Sec. IV.

## II. THE FUNCTIONAL MONTE CARLO METHOD

In this paper we consider a standard, planar geometry, monoenergetic  $k$ -eigenvalue problem with vacuum boundaries:

$$\mu \frac{\partial \psi}{\partial x}(x, \mu) + \Sigma_r(x)\psi(x, \mu) - \int_{-1}^1 \Sigma_s(x, \mu, \mu')\psi(x, \mu') d\mu' = \frac{\nu \Sigma_f(x)}{2k} \int_{-1}^1 \psi(x, \mu') d\mu', \quad 0 < x < X, \quad (1a)$$

$$\psi(0, \mu) = 0, \quad 0 < \mu \leq 1, \quad (1b)$$

and

$$\psi(X, \mu) = 0, \quad -1 \leq \mu < 0, \quad (1c)$$

where

$$\Sigma_s(x, \mu, \mu') = \sum_{n=0}^{\infty} \frac{2n+1}{2} \Sigma_{sn}(x) P_n(\mu) P_n(\mu'). \quad (2)$$

Equations (1) are the high-order transport equations for  $\psi(x, \mu)$  and  $k$ . The low-order FMC equations are derived by the following procedure:

*Step 1.* We construct specified angular moments of Eqs. (1). Specifically, we take the zeroth and first angular moments of Eq. (1a), and we multiply Eqs. (1b) and (1c) by  $\mu$  and integrate over the incident directions. No approximations are made in performing these operations, and the exact solution of Eqs. (1) satisfies the angularly integrated equations. (This step duplicates the first step of deriving the low-order QD equations.)

*Step 2.* Next, we define a spatial grid of  $J$  cells, we define  $J + 1$  “tent” functions on this grid, and using the tent functions, we construct certain spatial moments of the angularly integrated equations obtained in step 1. Again, no approximations are made in performing these operations, and the exact solution of Eqs. (1) satisfies these spatially and angularly integrated equations. (This step is not part of the QD method.)

*Step 3.* With no approximation, we manipulate the spatially and angularly integrated equations from step 2 to obtain a discrete system of low-order FMC equations, containing (a) nonlinear functionals of the exact solution and (b) spatial moments of the scalar flux around each of the  $J + 1$  grid points. (This step is patterned after the QD method.) Once again, no approximations are made in performing these operations. If the nonlinear functionals are known exactly, the discrete system yields exactly (a) the spatial moments of the scalar flux around each of the  $J + 1$  grid points and (b) the  $k$ -eigenvalue.

After deriving the low-order FMC equations, the Monte Carlo simulation of Eqs. (1) can begin. In the simulations generated for this paper, we used a very simple approach. Namely, we wrote a test code to implement the standard Monte Carlo simulation of the eigenvalue problem defined in Eqs. (1). In this standard implementation, the user specifies the number of Monte Carlo particles per generation; the simulation begins with a crude (flat) estimate of the fission source; inactive cycles (generations) are performed to converge the fission source; and then active cycles (generations) are performed to estimate the eigenfunction and  $k$ . All these operations are performed using conventional Monte Carlo procedures. The results of this process are the standard Monte Carlo results reported in Sec. III of this paper.

However, while performing these standard Monte Carlo operations, the information from the Monte Carlo particle histories is used to generate estimates of the scalar flux  $\phi$  (the eigenfunction) and of the nonlinear functionals in the low-order FMC equations. More specifically, for each active generation, we calculate new estimates of the FMC functionals, using the new data generated from the Monte Carlo histories processed during that generation. At the end of each generation, after all the fission Monte Carlo particles have been processed, the FMC functionals are calculated and the discrete low-order FMC equations are solved. This yields the FMC estimates of the  $k$ -eigenfunction and the  $k$ -eigenvalue for that generation. This process is repeated for each active generation. After a specified number of active generations, the mean value and standard deviation of the (standard Monte Carlo and FMC) generation-wise eigenvalues are calculated in the usual way.

In the simulations performed for this paper, the results of the FMC calculations do not affect the Monte Carlo simulation of Eqs. (1). The FMC calculations are performed using additional information extracted from the conventional Monte Carlo particle histories, but none of this new information impacts the Monte Carlo simulation of Eqs. (1). A more sophisticated approach might, for example, use the (generally more accurate) estimate of the fission source from the low-order FMC calculations to generate the fission source for the next generation. However, we did not do this in the numerical simulations reported here. The purpose of this paper is to describe the FMC method and show that even with a tilted or otherwise poorly represented Monte Carlo fission source, it can be much more accurate than standard Monte Carlo.

Because the FMC functionals are only weakly dependent on the angular flux  $\psi$ , the Monte Carlo estimates of these functionals are less noisy than those of  $\phi$ , and the FMC estimates of the eigenvalue and the eigenfunction generally have a smaller variance than the standard estimates. Also, because the standard Monte Carlo and FMC methods have only statistical errors, in the

limit of an infinite number of Monte Carlo particles per generation and an infinite number of generations, both methods will yield the exact eigenvalue and eigenfunction.

We now begin the derivation of the low-order FMC equations. Following step 1 described above, we take specified angular moments of Eqs. (1) and operate on Eq. (1a) by  $\int_{-1}^1 \mu^n(\cdot) d\mu$  for  $n = 0$  and 1. Defining

$$\phi_n(x) = \int_{-1}^1 \mu^n \psi(x, \mu) d\mu, \quad (3a)$$

$$\Sigma_a(x) = \Sigma_r(x) - \Sigma_{s0}(x), \quad (3b)$$

and

$$\Sigma_{tr}(x) = \Sigma_r(x) - \Sigma_{s1}(x), \quad (3c)$$

we obtain

$$\frac{d\phi_1}{dx}(x) + \Sigma_a(x)\phi_0(x) = \frac{\nu\Sigma_f(x)}{k}\phi_0(x) \quad (4a)$$

and

$$\frac{d\phi_2}{dx}(x) + \Sigma_{tr}(x)\phi_1(x) = 0. \quad (4b)$$

Also, operating on Eq. (1b) by  $\int_0^1 2\mu(\cdot) d\mu$  and on Eq. (1c) by  $\int_{-1}^0 2\mu(\cdot) d\mu$ , we obtain

$$0 = \phi_1(0) + \int_{-1}^1 |\mu| \psi(0, \mu) d\mu \quad (5a)$$

and

$$0 = \phi_1(X) - \int_{-1}^1 |\mu| \psi(X, \mu) d\mu. \quad (5b)$$

Solving Eq. (4b) for  $\phi_1(x)$ ,

$$\phi_1(x) = -\frac{1}{\Sigma_{tr}(x)} \frac{d\phi_2}{dx}(x), \quad (6)$$

and using this to eliminate  $\phi_1$  from Eqs. (4a) and (5), we obtain

$$\begin{aligned} -\frac{d}{dx} \frac{1}{\Sigma_{tr}(x)} \frac{d\phi_2}{dx}(x) + \Sigma_a(x)\phi_0(x) \\ = \frac{\nu\Sigma_f(x)}{k} \phi_0(x), \end{aligned} \quad (7a)$$

$$\frac{1}{\Sigma_{tr}(0)} \frac{d\phi_2}{dx}(0) = \int_{-1}^1 |\mu| \psi(0, \mu) d\mu, \quad (7b)$$

and

$$\frac{1}{\Sigma_{tr}(X)} \frac{d\phi_2}{dx}(X) = - \int_{-1}^1 |\mu| \psi(X, \mu) d\mu . \tag{7c}$$

Equations (7) are exactly satisfied by the solution of Eqs. (1). This completes step 1 of the derivation of the FMC equations.

Next, we perform step 2 described above. We prescribe a spatial grid, consisting of  $J + 1$  points  $x_{j+1/2}$  satisfying  $0 = x_{1/2} < x_{3/2} < \dots < x_{j-1/2} < x_{j+1/2} < \dots < x_{J-1/2} < x_{J+1/2} = X$ . The  $j$ 'th spatial cell consists of the interval  $x_{j-1/2} < x < x_{j+1/2}$ ; the width of this cell is  $h_j = x_{j+1/2} - x_{j-1/2}$ . On each  $j$ 'th spatial cell, the cross sections are assumed to be constant and are written as  $\Sigma_{tr}(x) = \Sigma_{tr,j}$ ,  $\Sigma_a(x) = \Sigma_{a,j}$ , and  $\nu\Sigma_f(x) = \nu\Sigma_{f,j}$ .

For  $0 \leq j \leq J$ , we define the following tent functions  $f_{j+1/2}(x)$ , which are depicted in Fig. 1. For  $j = 0$ ,

$$f_{1/2}(x) = \begin{cases} \frac{1}{h_1} (x_{3/2} - x) , & 0 = x_{1/2} < x < x_{3/2} \\ 0 , & \text{otherwise} , \end{cases} \tag{8a}$$

for  $1 \leq j \leq J - 1$ ,

$$f_{j+1/2}(x) = \begin{cases} \frac{1}{h_j} (x - x_{j-1/2}) , & x_{j-1/2} < x < x_{j+1/2} \\ \frac{1}{h_{j+1}} (x_{j+3/2} - x) , & x_{j+1/2} < x < x_{j+3/2} \\ 0 , & \text{otherwise} , \end{cases} \tag{8b}$$

and for  $j = J$ ,

$$f_{J+1/2}(x) = \begin{cases} \frac{1}{h_J} (x - x_{J-1/2}) , & x_{J-1/2} < x < x_{J+1/2} = X \\ 0 , & \text{otherwise} . \end{cases} \tag{8c}$$

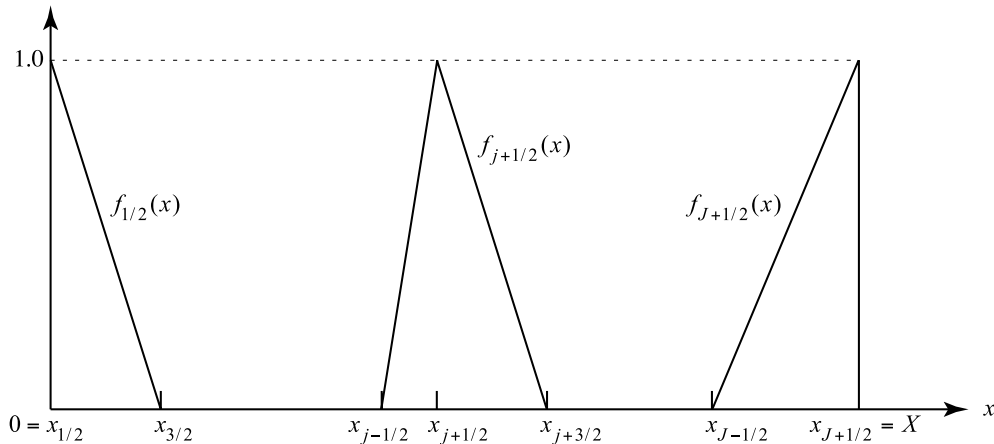


Fig. 1. Spatial grid and tent functions.



Next, we multiply Eq. (7a) by  $f_{j+1/2}(x)$  and integrate over  $0 \leq x \leq X$ . For  $j = 0$  we obtain

$$\begin{aligned} & - \int_{x_{1/2}}^{x_{3/2}} f_{1/2}(x) \left[ \frac{d}{dx} \frac{1}{\Sigma_{tr}(x)} \frac{d\phi_2}{dx}(x) \right] dx \\ & + \int_{x_{1/2}}^{x_{3/2}} f_{1/2}(x) \Sigma_a(x) \phi_0(x) dx \\ & = \frac{1}{k} \int_{x_{1/2}}^{x_{3/2}} f_{1/2}(x) \nu \Sigma_f(x) \phi_0(x) dx . \end{aligned}$$

Integrating the first term by parts and using Eq. (7b), we obtain

$$\begin{aligned} & \int_{x_{1/2}}^{x_{3/2}} f_{1/2}(x) \left[ \frac{d}{dx} \frac{1}{\Sigma_{tr}(x)} \frac{d\phi_2}{dx}(x) \right] dx \\ & = f_{1/2}(x) \frac{1}{\Sigma_{tr,1}} \frac{d\phi_2}{dx}(x) \Big|_{x_{1/2}}^{x_{3/2}} \\ & - \int_{x_{1/2}}^{x_{3/2}} \frac{df_{1/2}}{dx}(x) \frac{1}{\Sigma_{tr,1}} \frac{d\phi_2}{dx}(x) dx \\ & = - \frac{1}{\Sigma_{tr,1}} \frac{d\phi_2}{dx}(0) + \frac{1}{\Sigma_{tr,1} h_1} \int_{x_{1/2}}^{x_{3/2}} \frac{d\phi_2}{dx}(x) dx \\ & = - \int_{-1}^1 |\mu| \psi(x_{1/2}, \mu) d\mu \\ & + \frac{1}{\Sigma_{tr,1} h_1} [\phi_2(x_{3/2}) - \phi_2(x_{1/2})] . \end{aligned}$$

Thus, the preceding equation can be written:

$$\begin{aligned} & \int_{-1}^1 |\mu| \psi(x_{1/2}, \mu) d\mu - \frac{1}{\Sigma_{tr,1} h_1} [\phi_2(x_{3/2}) - \phi_2(x_{1/2})] \\ & + \int_{x_{1/2}}^{x_{3/2}} f_{1/2}(x) \Sigma_{a,1} \phi_0(x) dx \\ & = \frac{1}{k} \int_{x_{1/2}}^{x_{3/2}} f_{1/2}(x) \nu \Sigma_{f,1} \phi_0(x) dx . \end{aligned} \tag{9a}$$

For  $1 \leq j \leq J - 1$  we obtain

$$\begin{aligned} & - \int_{x_{j-1/2}}^{x_{j+3/2}} f_{j+1/2}(x) \left[ \frac{d}{dx} \frac{1}{\Sigma_{tr}(x)} \frac{d\phi_2}{dx}(x) \right] dx \\ & + \int_{x_{j-1/2}}^{x_{j+3/2}} f_{j+1/2}(x) \Sigma_a(x) \phi_0(x) dx \\ & = \frac{1}{k} \int_{x_{j-1/2}}^{x_{j+3/2}} f_{j+1/2}(x) \nu \Sigma_f(x) \phi_0(x) dx . \end{aligned}$$

Integrating the first term by parts, we obtain

$$\begin{aligned} & \int_{x_{j-1/2}}^{x_{j+3/2}} f_{j+1/2}(x) \left[ \frac{d}{dx} \frac{1}{\Sigma_{tr}(x)} \frac{d\phi_2}{dx}(x) \right] dx \\ & = - \int_{x_{j-1/2}}^{x_{j+3/2}} \frac{df_{j+1/2}}{dx}(x) \frac{1}{\Sigma_{tr}(x)} \frac{d\phi_2}{dx}(x) dx \\ & = - \int_{x_{j-1/2}}^{x_{j+1/2}} \frac{1}{h_j \Sigma_{tr,j}} \frac{d\phi_2}{dx}(x) dx \\ & + \int_{x_{j+1/2}}^{x_{j+3/2}} \frac{1}{h_{j+1} \Sigma_{tr,j+1}} \frac{d\phi_2}{dx}(x) dx \\ & = \frac{1}{\Sigma_{tr,j+1} h_{j+1}} [\phi_2(x_{j+3/2}) - \phi_2(x_{j+1/2})] \\ & - \frac{1}{\Sigma_{tr,j} h_j} [\phi_2(x_{j+1/2}) - \phi_2(x_{j-1/2})] . \end{aligned}$$

Thus, the preceding equation can be written

$$\begin{aligned} & - \frac{1}{\Sigma_{tr,j+1} h_{j+1}} [\phi_2(x_{j+3/2}) - \phi_2(x_{j+1/2})] \\ & + \frac{1}{\Sigma_{tr,j} h_j} [\phi_2(x_{j+1/2}) - \phi_2(x_{j-1/2})] \\ & + \int_{x_{j-1/2}}^{x_{j+3/2}} f_{j+1/2}(x) \Sigma_a(x) \phi_0(x) dx \\ & = \frac{1}{k} \int_{x_{j-1/2}}^{x_{j+3/2}} f_{j+1/2}(x) \nu \Sigma_f(x) \phi_0(x) dx . \end{aligned} \tag{9b}$$

For  $j = J$  we follow similar steps as for  $j = 0$  and obtain

$$\begin{aligned} & \int_{-1}^1 |\mu| \psi(x_{J+1/2}, \mu) d\mu \\ & + \frac{1}{\Sigma_{tr,J} h_J} [\phi_2(x_{J+1/2}) - \phi_2(x_{J-1/2})] \\ & + \int_{x_{J-1/2}}^{x_{J+1/2}} f_{J+1/2}(x) \Sigma_{a,J} \phi_0(x) dx \\ & = \frac{1}{k} \int_{x_{J-1/2}}^{x_{J+1/2}} f_{J+1/2}(x) \nu \Sigma_{f,J} \phi_0(x) dx . \end{aligned} \tag{9c}$$

Equations (9) are a system of  $J + 1$  discrete equations, which are exactly satisfied by the solution  $\psi(x, \mu)$  and  $k$  of Eqs. (1). This completes step 2 of the derivation of the FMC equations.

Next, we perform step 3 described above. For each  $0 \leq j \leq J$ , we introduce new functions  $g_{j+1/2}(x)$  that are nonzero only where  $f_{j+1/2}(x)$  are nonzero. These functions are not uniquely defined; there is considerable flexibility in choosing them. In this paper we use two definitions of  $g_{j+1/2}(x)$ . First, we use a delta-function definition:

$$g_{j+1/2}(x) = \delta(x - x_{j+1/2}) , \quad 0 \leq j \leq J . \quad (10)$$

We also use a histogram definition. With  $x_j = (x_{j+1/2} + x_{j-1/2})/2 =$  midpoint of the  $j$ 'th spatial cell, we define for  $j = 0$ ,

$$g_{1/2}(x) = \begin{cases} \frac{2}{h_1} , & x_{1/2} \leq x \leq x_1 , \\ 0 , & \text{otherwise} , \end{cases} \quad (11a)$$

for  $1 \leq j \leq J - 1$ ,

$$g_{j+1/2}(x) = \begin{cases} \frac{2}{h_j + h_{j+1}} , & x_j \leq x \leq x_{j+1} , \\ 0 , & \text{otherwise} , \end{cases} \quad (11b)$$

and for  $j = J$ ,

$$g_{J+1/2}(x) = \begin{cases} \frac{2}{h_J} , & x_J \leq x \leq x_{J+1/2} , \\ 0 , & \text{otherwise} . \end{cases} \quad (11c)$$

Other definitions of  $g_{j+1/2}$  are possible; for example,  $g_{j+1/2} = f_{j+1/2}$ . However, these will not be considered in this paper.

For  $0 \leq j \leq J$ , we define

$$\Phi_{j+1/2} = \int_{x_{j-1/2}}^{x_{j+3/2}} g_{j+1/2}(x) \phi_0(x) dx , \quad (12)$$

where  $\phi_0(x)$  is the scalar flux,  $x_{-1/2} = x_{1/2} = 0$ , and  $x_{J+3/2} = x_{J+1/2} = X$ . The quantities  $\Phi_{j+1/2}$  will be the flux unknowns in the low-order FMC equations. If Eq. (10) is used to define  $g_{j+1/2}(x)$ , then for  $0 \leq j \leq J$ ,

$$\begin{aligned} \Phi_{j+1/2} &= \phi_0(x_{j+1/2}) \\ &= \text{pointwise (cell-edge) scalar flux at } x_{j+1/2} . \end{aligned}$$

If Eqs. (11) are used to define  $g_{j+1/2}(x)$ , then for  $1 \leq j \leq J - 1$ ,

$$\begin{aligned} \Phi_{j+1/2} &= \frac{2}{h_j + h_{j+1}} \int_{x_j}^{x_{j+1}} \phi_0(x) dx \\ &= \text{scalar flux averaged between the} \\ &\quad \text{midpoints of the } j\text{'th and } (j + 1)\text{st cells} . \end{aligned}$$

In the remainder of this paper we refer to the  $\Phi_{j+1/2}$  obtained using  $g_{j+1/2}$  defined by Eq. (10) as the *edge* unknowns, and to the  $\Phi_{j+1/2}$  obtained using  $g_{j+1/2}$  defined by Eq. (11) as the *average* unknowns.

To proceed, we multiply and divide each of the terms in Eqs. (9) by a suitable  $\Phi_{j+1/2}$  to obtain the following equivalent system of  $J + 1$  equations:

$$\begin{aligned} &\left[ \frac{\int_{-1}^1 |\mu| \psi(x_{1/2}, \mu) d\mu}{\Phi_{1/2}} + \frac{1}{\Sigma_{tr,1} h_1} \frac{\phi_2(x_{1/2})}{\Phi_{1/2}} + \frac{\int_{x_{1/2}}^{x_{3/2}} f_{1/2}(x) \Sigma_{a,1} \phi_0(x) dx}{\Phi_{1/2}} \right] \Phi_{1/2} \\ &\quad - \left[ \frac{1}{\Sigma_{tr,1} h_1} \frac{\phi_2(x_{3/2})}{\Phi_{3/2}} \right] \Phi_{3/2} = \frac{1}{k} \left[ \frac{\int_{x_{1/2}}^{x_{3/2}} f_{1/2}(x) \nu \Sigma_{f,1} \phi_0(x) dx}{\Phi_{1/2}} \right] \Phi_{1/2} , \end{aligned} \quad (13a)$$

$$\begin{aligned} &\left[ \left( \frac{1}{\Sigma_{tr,\{j+1\}} h_{j+1}} + \frac{1}{\Sigma_{tr,j} h_j} \right) \frac{\phi_2(x_{j+1/2})}{\Phi_{j+1/2}} + \frac{\int_{x_{j-1/2}}^{x_{j+3/2}} f_{j+1/2}(x) \Sigma_a(x) \phi_0(x) dx}{\Phi_{j+1/2}} \right] \Phi_{j+1/2} \\ &\quad - \left[ \frac{1}{\Sigma_{tr,j} h_j} \frac{\phi_2(x_{j-1/2})}{\Phi_{j-1/2}} \right] \Phi_{j-1/2} - \left[ \frac{1}{\Sigma_{tr,j+1} h_{j+1}} \frac{\phi_2(x_{j+3/2})}{\Phi_{j+3/2}} \right] \Phi_{j+3/2} \\ &= \frac{1}{k} \left[ \frac{\int_{x_{j-1/2}}^{x_{j+3/2}} f_{j+1/2}(x) \nu \Sigma_f(x) \phi_0(x) dx}{\Phi_{j+1/2}} \right] \Phi_{j+1/2} , \quad 1 \leq j \leq J - 1 , \end{aligned} \quad (13b)$$

and

$$\begin{aligned} &\left[ \frac{\int_{-1}^1 |\mu| \psi(x_{J+1/2}, \mu) d\mu}{\Phi_{J+1/2}} + \frac{1}{\Sigma_{tr,J} h_J} \frac{\phi_2(x_{J+1/2})}{\Phi_{J+1/2}} + \frac{\int_{x_{J-1/2}}^{x_{J+1/2}} f_{J+1/2}(x) \Sigma_{a,J} \phi_0(x) dx}{\Phi_{J+1/2}} \right] \Phi_{J+1/2} \\ &\quad - \left[ \frac{1}{\Sigma_{tr,J} h_J} \frac{\phi_2(x_{J-1/2})}{\Phi_{J-1/2}} \right] \Phi_{J-1/2} = \frac{1}{k} \left[ \frac{\int_{x_{J-1/2}}^{x_{J+1/2}} f_{J+1/2}(x) \nu \Sigma_{f,J} \phi_0(x) dx}{\Phi_{J+1/2}} \right] \Phi_{J+1/2} . \end{aligned} \quad (13c)$$

Equivalently, if we define the following nonlinear functionals of  $\psi$ :

$$B_{1/2} = \frac{\int_{-1}^1 |\mu| \psi(x_{1/2}, \mu) d\mu}{\int_{x_{1/2}}^{x_{3/2}} \int_{-1}^1 g_{1/2}(x) \psi(x, \mu) d\mu dx}, \quad (14a)$$

$$B_{J+1/2} = \frac{\int_{-1}^1 |\mu| \psi(x_{J+1/2}, \mu) d\mu}{\int_{x_{J-1/2}}^{x_{J+3/2}} \int_{-1}^1 g_{J+1/2}(x) \psi(x, \mu) d\mu dx}, \quad (14b)$$

$$E_{j+1/2} = \frac{\int_{-1}^1 \mu^2 \psi(x_{j+1/2}, \mu) d\mu}{\int_{x_{j-1/2}}^{x_{j+3/2}} \int_{-1}^1 g_{j+1/2}(x) \psi(x, \mu) d\mu dx}, \quad (14c)$$

$$A_{j+1/2} = \frac{\int_{x_{j-1/2}}^{x_{j+3/2}} f_{j+1/2}(x) \Sigma_a(x) \phi_0(x) dx}{\int_{x_{j-1/2}}^{x_{j+3/2}} g_{j+1/2}(x) \phi_0(x) dx}, \quad (14d)$$

and

$$F_{j+1/2} = \frac{\int_{x_{j-1/2}}^{x_{j+3/2}} f_{j+1/2}(x) \nu \Sigma_f(x) \phi_0(x) dx}{\int_{x_{j-1/2}}^{x_{j+3/2}} g_{j+1/2}(x) \phi_0(x) dx}, \quad (14e)$$

then Eqs. (13) can be written more compactly as

$$\begin{aligned} & \left[ B_{1/2} + \frac{1}{\Sigma_{tr,1} h_1} E_{1/2} + A_{1/2} \right] \Phi_{1/2} \\ & - \left[ \frac{1}{\Sigma_{tr,1} h_1} E_{3/2} \right] \Phi_{3/2} \\ & = \frac{1}{k} [F_{1/2}] \Phi_{1/2}, \end{aligned} \quad (15a)$$

$$\begin{aligned} & \left[ \left( \frac{1}{\Sigma_{tr,j} h_j} + \frac{1}{\Sigma_{tr,j+1} h_{j+1}} \right) E_{j+1/2} + A_{j+1/2} \right] \Phi_{j+1/2} \\ & - \left[ \frac{1}{\Sigma_{tr,j} h_j} E_{j-1/2} \right] \Phi_{j-1/2} \\ & - \left[ \frac{1}{\Sigma_{tr,j+1} h_{j+1}} E_{j+3/2} \right] \Phi_{j+3/2} \\ & = \frac{1}{k} [F_{j+1/2}] \Phi_{1/2}, \quad 1 \leq j \leq J-1, \end{aligned} \quad (15b)$$

and

$$\begin{aligned} & \left[ B_{J+1/2} + \frac{1}{\Sigma_{tr,J} h_J} E_{J+1/2} + A_{J+1/2} \right] \Phi_{J+1/2} \\ & - \left[ \frac{1}{\Sigma_{tr,J} h_J} E_{J-1/2} \right] \Phi_{J-1/2} \\ & = \frac{1}{k} [F_{J+1/2}] \Phi_{J+1/2}. \end{aligned} \quad (15c)$$

Equations (14) and (15) are exactly satisfied by solution  $\psi(x, \mu)$  and  $k$  of Eqs. (1). However, the following is also true: If the functionals in Eqs. (14) are evaluated using the exact eigenfunction  $\psi(x, \mu)$  and Eqs. (15) are then solved for  $\Phi_{j+1/2}$  and  $k$ , then the resulting  $\Phi_{j+1/2}$  and  $k$  are *exact*, i.e.,  $k$  is the exact eigenvalue, and  $\Phi_{j+1/2}$  are the exact appropriate space-angle moments of  $\psi$ . [We remark that the QD method has boundary and Eddington factor functionals that are closely related to the  $B$  and  $E$  functionals in Eqs. (14).]

To summarize the FMC procedure used in this paper, Eqs. (1) are simulated using the standard Monte Carlo method of processing fission particles from one cycle to the next. The standard Monte Carlo  $k$ -eigenvalue is estimated for each cycle, and the final (standard Monte Carlo) estimate of  $k$  is obtained by averaging  $k$  over all active cycles. During this process, additional information is processed and stored beyond what is needed to perform the standard simulation. Specifically, Monte Carlo estimates of each of the integrals in the numerators and denominators of Eqs. (14) are obtained. At the end of each active cycle, the functionals in Eqs. (14) are calculated, and Eqs. (15) are solved to obtain the FMC cycle-wise estimates of  $\Phi_{j+1/2}$  and  $k$ . After the active cycles are completed, the FMC eigenvalues are averaged over the active cycles to obtain the final FMC estimate of  $k$ . In the simulations for this paper, results from the low-order FMC calculations do not modify the high-order Monte Carlo simulations of Eqs. (1).

The FMC method is based on two assumptions:

1. The functionals in Eqs. (14) depend weakly on  $\psi$  and can be evaluated with Monte Carlo more accurately than direct Monte Carlo estimates of  $\phi_0$  and  $k$ .

2. If Eqs. (15) are solved with small errors in the functionals, the resulting errors in  $\Phi_{j+1/2}$  and  $k$  will be small.

To argue the first point, we note that the functionals in Eqs. (14) are all local, e.g.,  $E_{j+1/2}$  depends on estimates of  $\psi$  only in the  $j$ 'th and  $(j+1)$ th spatial cells. Also, these functionals depend only on low-order spatial and angular moments of  $\psi$ , and because of their nonlinear character, they are weakly dependent on the amplitude of  $\psi$ . Therefore, if a Monte Carlo estimate of  $\psi$  has a poor estimate of the amplitude but a reasonably good

estimate of the spatial and angular shape of  $\psi$ , then the functionals in Eqs. (14) should be evaluated accurately.

To argue the second point, if we use the crude estimate of  $\psi$ ,

$$\psi(x, \mu) \approx \frac{\phi_{0,j+1/2}}{2}, \quad x_{j-1/2} < x < x_{j+1/2} \quad (16)$$

in Eqs. (14), we obtain

$$B_{1/2} = B_{J+1/2} = \frac{1}{2}, \quad (17a)$$

$$E_{j+1/2} = \frac{1}{3}, \quad (17b)$$

$$A_{j+1/2} = \begin{cases} \frac{1}{2} \Sigma_{a,1} h_1, & j = 0 \\ \frac{1}{2} (\Sigma_{a,j} h_j + \Sigma_{a,j+1} h_{j+1}), & 1 \leq j \leq J-1 \\ \frac{1}{2} \Sigma_{a,J} h_J, & j = J, \end{cases} \quad (17c)$$

and

$$F_{j+1/2} = \begin{cases} \frac{1}{2} \nu \Sigma_{f,1} h_1, & j = 0 \\ \frac{1}{2} (\nu \Sigma_{f,j} h_j + \nu \Sigma_{f,j+1} h_{j+1}), & 1 \leq j \leq J-1 \\ \frac{1}{2} \nu \Sigma_{f,J} h_J, & j = J. \end{cases} \quad (17d)$$

When these functional values—all of which are independent of  $\phi_{0,j+1/2}$ —are introduced into Eqs. (15), we obtain the standard cell-edge diffusion discretization of the diffusion approximation to Eqs. (1).

Thus, the discrete system of Eqs. (15) is closely related to the classic diffusion approximation to Eqs. (1). If the underlying physical transport problem has eigenfunctions and the eigenvalues that are weakly sensitive to small perturbations in the fuel or moderator, then small statistical errors in the FMC functionals should produce comparably small statistical errors in the FMC estimates of the eigenfunction and the eigenvalue.

However, there are physical problems in which the eigenfunction is highly sensitive to small perturbations in the fuel or moderator. For example, an infinite periodic system consisting of identical widely separated fissile regions will have a spatially periodic eigenfunction. If in one of the fissile regions  $\nu \Sigma_f$  is increased slightly,

then (a) the eigenfunction will change markedly, acquiring a large peak at the location of the special fissile region, but (b) the eigenvalue will change only slightly. For such problems, the low-order FMC equations should be sensitive to small (statistical) errors in the nonlinear functionals, resulting in FMC eigenfunction estimates that have large estimated standard deviations. However, the FMC eigenvalue estimates should have much smaller estimated standard deviations.

Because Monte Carlo estimates of the integrals in the denominators of Eqs. (14) are noisier for the edge definitions of  $g_{j+1/2}$  [Eq. (10)] than for the average definitions [Eqs. (11)], the FMC edge estimates of the nonlinear functionals should be noisier than the average estimates. In our numerical simulations, we show that indeed this is the case, and that this yields noisier edge FMC eigenfunctions than average FMC eigenfunctions. Nonetheless, somewhat surprisingly, we observe the edge and average estimates of the eigenvalues to be of comparable quality.

Next, we test the FMC method as described above on three problems for which the standard Monte Carlo method is problematic. These problems have been chosen to highlight the strengths and the weaknesses of the FMC method.

### III. NUMERICAL RESULTS

First, we consider a relatively straightforward problem of a large homogeneous fissile region surrounded by a thin reflector. The physical data is given in Table I. For all three problems discussed in this paper,  $x$  has units of centimeters,  $\Sigma$  has units of  $\text{cm}^{-1}$ , in column 5 of the data tables  $n = 1, 2, 3$ , and  $\Sigma_{s,n} = 0$  for  $n \geq 4$ . In problem 1, the exact eigenfunction has a basic cosine shape in the central fissile region. Our fine-mesh  $S_N$  solution of this problem, which used the  $S_{32}$  Gauss-Legendre quadrature set with  $h = 0.01$ , produced  $k = 0.999384$ . Our Monte Carlo simulations of this problem used 50 000 histories per cycle with a uniform grid  $h = 1.0$ .

We began all our Monte Carlo simulations with a flat fission source. In Fig. 2, we display the problem 1  $S_N$  eigenfunction and averaged estimates of the eigenfunction from (a) standard Monte Carlo, (b) FMC using the

TABLE I  
Data for Problem 1

Region	Location	$\Sigma_t$	$\Sigma_{s,0}$	$\Sigma_{s,n}$	$\nu \Sigma_f$
1	$0 < x < 5$	1.0	0.856	0.1	0
2	$5 < x < 205$	1.0	0.856	0.1	0.144
3	$205 < x < 210$	1.0	0.856	0.1	0

FUNCTIONAL MONTE CARLO FOR  $k$ -EIGENVALUE

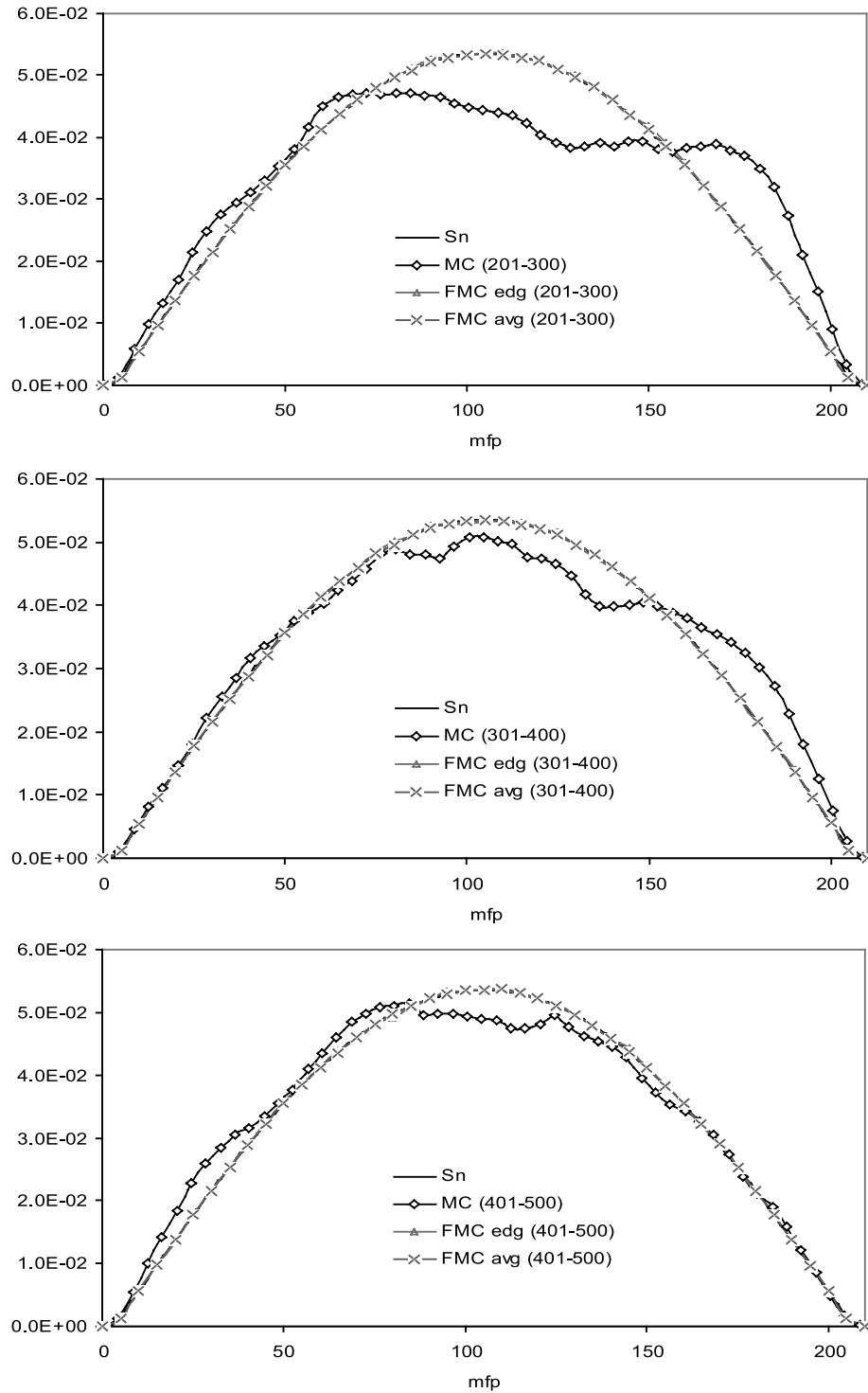


Fig. 2. Averaged problem 1 eigenfunction estimates during cycles 201 to 500.

edge unknowns (FMC edge), and (c) FMC using the averaged unknowns (FMC avg). As indicated in Fig. 2, these plots are obtained by averaging the Monte Carlo estimates of the eigenfunction over cycles 201 to 300, 301 to 400, and 401 to 500.

Figure 2 shows that the  $S_N$  and FMC estimates of the eigenfunction are virtually coincident and are much more accurate than the Monte Carlo estimates. The Monte Carlo eigenfunction appears to be trying to converge to the correct cosine shape but somewhat erratically. Based on

these results, we decided to take the first 500 cycles to be inactive and to process 500 more active cycles.

Figure 3 displays information concerning eigenfunction estimates at the 500'th cycle, just prior to the beginning of the active cycles. Figure 3 shows that, as expected, the Monte Carlo estimates of the nonlinear functionals  $E$  and  $A$  are much more accurate than the direct Monte Carlo estimate of the eigenfunction, and the average FMC functionals are less noisy than the edge functionals. Also, the Monte Carlo eigenfunction estimate is noisier than the FMC edge eigenfunction estimate, which in turn is noisier than the FMC average eigenfunction estimate. (These observations are valid for all fission cycles, both inactive and active.)

Figure 4 shows similar data as in Fig. 2, but now for 300 of the 500 active cycles. Again, the  $S_N$  and FMC estimates of the eigenfunction are virtually coincident and much more accurate than the Monte Carlo estimates. Also, the Monte Carlo eigenfunction estimate, which during the inactive cycles appeared to be converging toward the correct cosine shape, now slowly wobbles away from it. This wobbling is caused by undersampling of the fission source and can be suppressed by increasing the number of Monte Carlo particles per cycle.

Figure 5 shows the Monte Carlo estimates of the eigenfunction, averaged over the 500 active cycles (501 to 1000), and the estimated standard deviations in the Monte Carlo, FMC edge, and FMC average scalar fluxes over the active cycles. Figure 5 shows that even though it is averaged over a large number of active cycles, the Monte Carlo estimate of the eigenfunction is inaccurate and tilted. Because of the correlations in the fission source between one cycle and the next, the estimated standard deviations in the Monte Carlo eigenfunction shown in the bottom half of Fig. 5 are known to be unreliably low estimates of the true standard deviation. The extent to which these correlations affect the FMC estimates is not known. Nonetheless, the estimated standard deviations in the FMC eigenfunctions are smaller than those of the Monte Carlo eigenfunction, and the FMC eigenfunction estimates are clearly much more accurate.

We note from Fig. 3 that for individual cycles, the Monte Carlo and FMC estimates of the eigenfunction all contain high-frequency spatial errors, and from Figs. 2, 4, and 5 that by averaging these eigenfunction estimates over 100 or more cycles, the high-frequency errors are greatly suppressed. However, the Monte Carlo eigenfunction estimates contain much larger low-frequency errors than the FMC eigenfunction estimates, and these are not greatly suppressed by averaging over active cycles.

In Table II we display the estimates of the problem 1 eigenvalue during each of the ten 100-cycle spans (both active and inactive) that we ran. Table II shows that the FMC estimates of  $k$  are several orders of magnitude more accurate than the Monte Carlo estimates; this is due to

(a) the insensitivity of the nonlinear functionals to statistical errors in the flux estimates, (b) the insensitivity of the low-order FMC equations to small errors in the functionals, and (c) the relative geometric simplicity of the problem. An unexpected result is that even though the FMC-edge eigenfunction estimate is noisier than the FMC-average eigenfunction estimates, the two eigenvalue estimates are of comparable quality. This result holds consistently for all our simulations, and at the present time, we cannot offer an explanation. For more complex problems, we will show that the FMC edge and average estimates of the eigenvalue again are of comparable quality and remain more accurate than the standard Monte Carlo estimates, but not by the wide margin seen in this problem.

Next we consider two related problems, each having two slightly different fissile regions separated and surrounded by an absorbing moderator. The purpose of these problems is to examine the Monte Carlo and FMC methods when fissile regions begin to decouple. In problem 2, the two fissile regions are (a) separated by a 7-cm moderator and (b) surrounded by equivalent 5.0-cm moderators. The data for this problem is given in Table III. As in problem 1, column 5 holds for  $n = 1, 2$ , and 3, with  $\Sigma_{s,n} = 0$  for  $n \geq 4$ . The entire system is 27 cm thick. The  $S_{32}$  solution, obtained with  $h = 0.01$ , yielded  $k = 0.992429$ . Because of the slight (0.43%) asymmetry in  $\nu\Sigma_f$ , the  $S_N$  eigenfunction is asymmetric about the midpoint of the system; the peak of the eigenfunction in the right slightly more fissile region is nearly double that in the left fissile region. Our Monte Carlo simulations used 100 000 histories per cycle with a uniform grid  $h = 0.1$ .

In our simulation of this problem, the Monte Carlo estimate of the fission source seemed to converge near cycle 300. In Fig. 6, we show plots obtained by averaging the Monte Carlo and FMC estimates of the eigenfunction over cycles 201 to 300, 301 to 400, and 401 to 500. As in problem 1, the  $S_N$  and FMC eigenfunction estimates are virtually coincident. The Monte Carlo eigenfunction seems almost converged during cycles 301 to 400, but then it begins to drift away during cycles 401 to 500. (This drifting away from the converged solution also happened in problem 1.)

In Fig. 7 we show problem 2 eigenfunction plots for cycles 500, 501, and 502. As in problem 1, the correlations that exist between cycles cause the Monte Carlo estimate of the eigenfunction to change only slowly from one cycle to the next. Because the system is sensitive to perturbations in the cross sections (a 0.43% change in  $\nu\Sigma_f$  in one region causes a factor of 2 change in the eigenfunction), the FMC estimates of the eigenfunction show considerable variation from cycle to cycle. In Table IV, we present the estimates of the problem 2 eigenvalue during each of the ten 100-cycle spans that we ran. Table IV shows that estimated standard deviations in the FMC estimates of  $k$  are about a factor of 6 smaller

FUNCTIONAL MONTE CARLO FOR  $k$ -EIGENVALUE

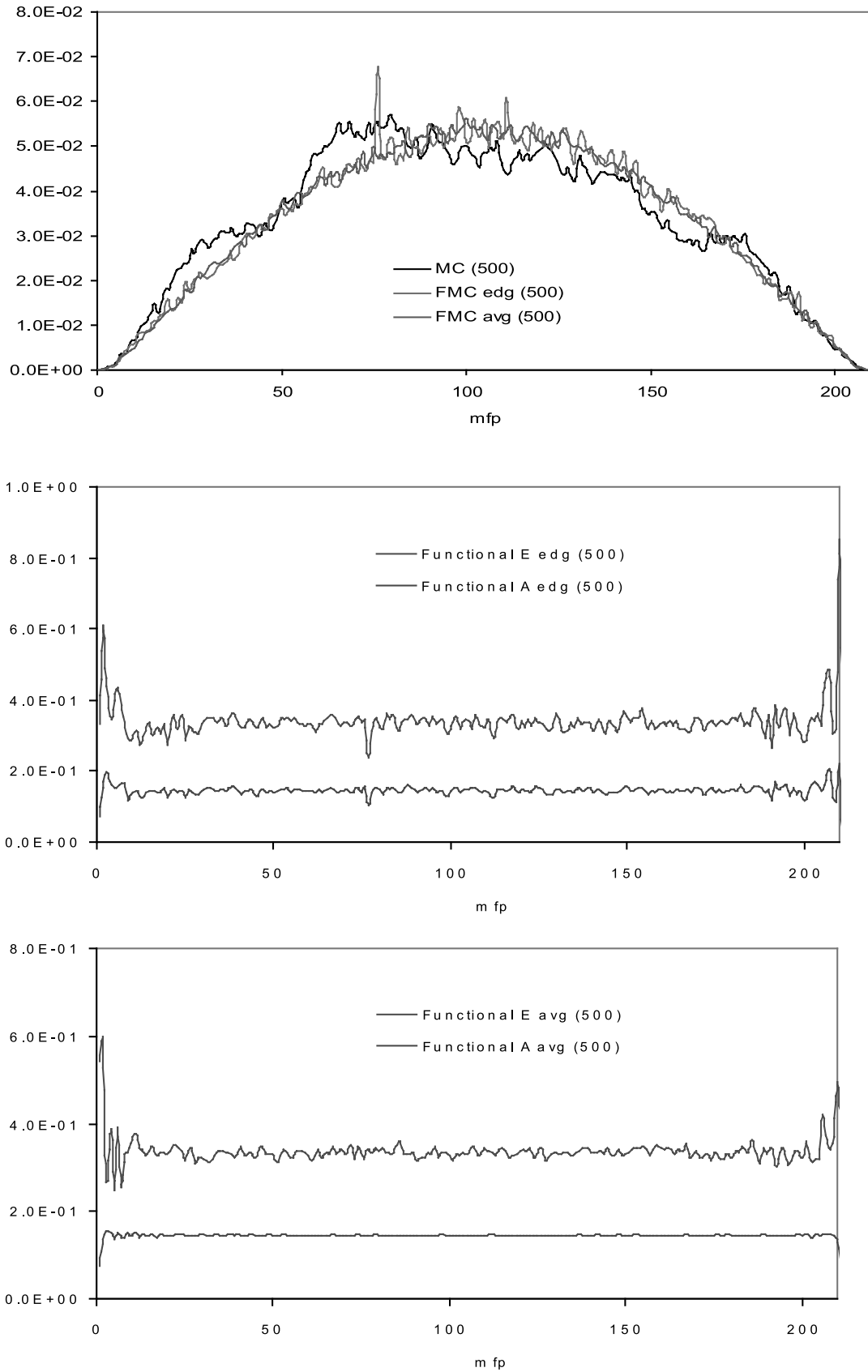


Fig. 3. Problem 1 eigenfunction and functional estimates for cycle 500.

LARSEN and YANG

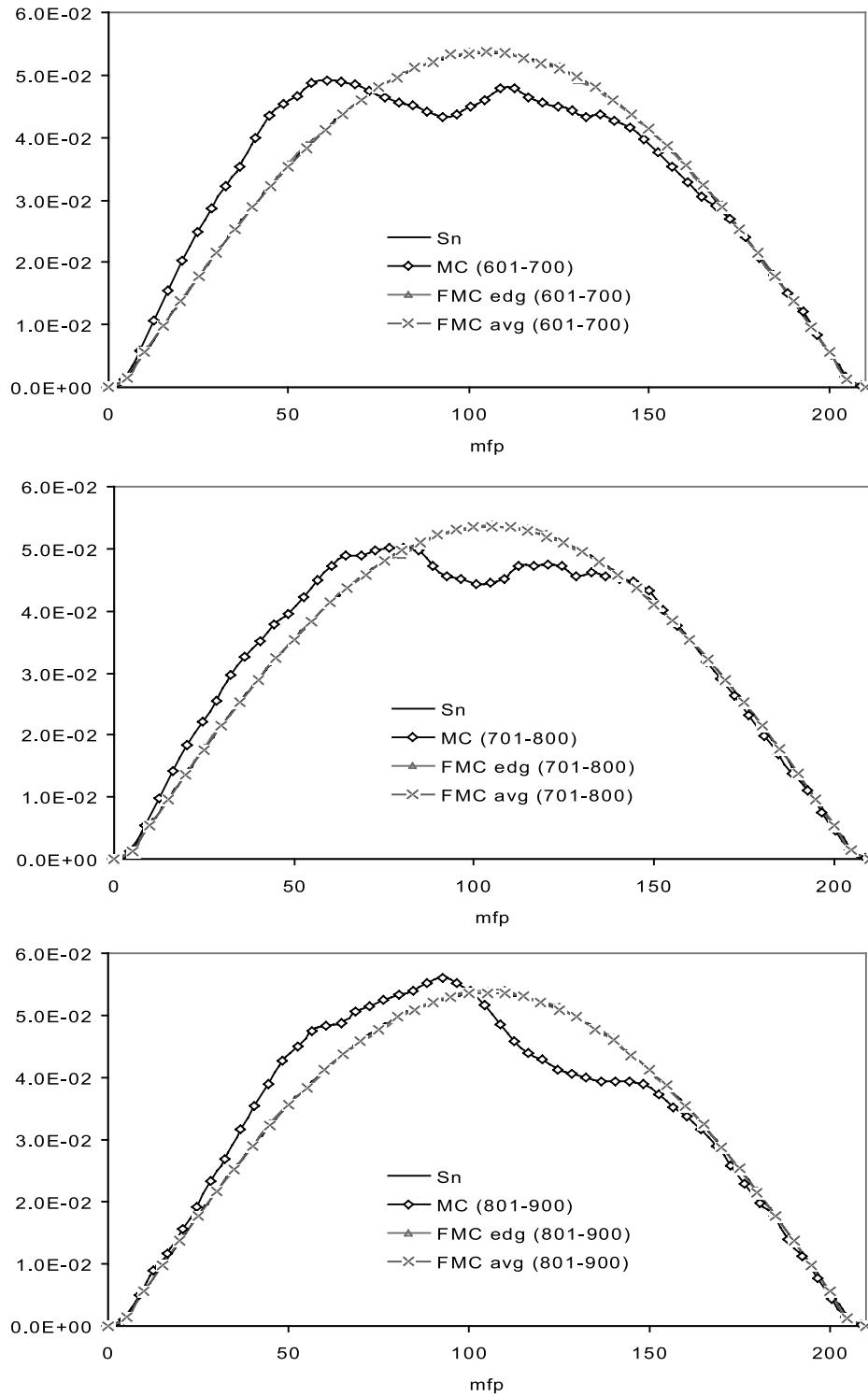


Fig. 4. Averaged problem 1 eigenfunction estimates during cycles 601 to 900.

than the Monte Carlo estimates. The errors in the FMC estimates of  $k$  (obtained by comparing to the  $S_N$  estimate) are smaller than the Monte Carlo estimates by a similar margin. This happens even though the FMC eigenfunc-

tion estimates have greater cycle-to-cycle variation than the Monte Carlo estimates. (But, Fig. 6 shows that the FMC eigenfunctions averaged over 100 cycles are more accurate than the Monte Carlo eigenfunctions.)



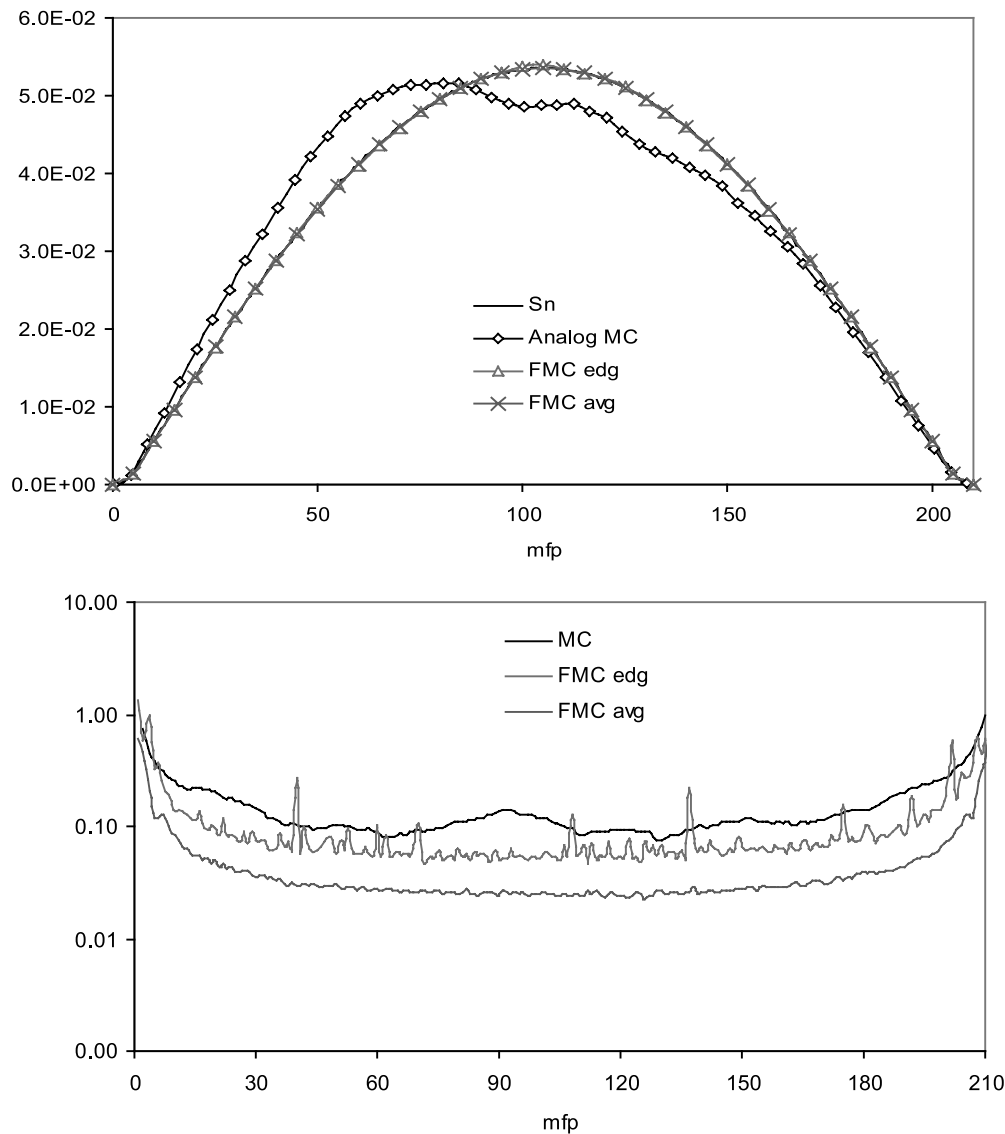
FUNCTIONAL MONTE CARLO FOR  $k$ -EIGENVALUE

Fig. 5. Problem 1 estimated mean eigenfunction and standard deviation over the 500 active cycles.

Problem 3 is similar to but more difficult than problem 2. The two fissile regions are now separated by a wider 10-cm absorbing moderator, and now a smaller (0.073%) increase in  $\nu\Sigma_f$  in the right fissile region yields an eigenfunction with a factor of 2 difference in the peaks at the two fissile regions. The data for this problem are given in Table V. Again, column 5 holds for  $n = 1, 2$ , and 3; with  $\Sigma_{s,n} = 0$  for  $n \geq 4$ . The entire system is 30 cm thick. The  $S_{32}$  solution, obtained with  $h = 0.01$ , yielded  $k = 0.987828$ . Our Monte Carlo simulations of this problem used 100,000 histories per cycle with a uniform grid  $h = 0.1$ .

In Fig. 8 we show plots obtained by averaging the Monte Carlo and FMC estimates of the eigenfunction over cycles 201 to 300, 301 to 400, and 401 to 500. For this problem the two FMC eigenfunction plots are very

similar to each other but are not as close to the  $S_N$  eigenfunction as they were in problem 2. However, the errors in the FMC eigenfunctions (compared to the  $S_N$  eigenfunction) are much smaller than the errors in the Monte Carlo eigenfunctions.

In Fig. 9, we show eigenfunction plots for cycles 500, 501, and 502. As in problem 2, the Monte Carlo eigenfunction estimate changes slowly from one cycle to the next, while now the FMC eigenfunction estimates vary more from cycle to cycle than in problem 2. This happens because the system is more sensitive to perturbations in the cross sections than in problem 2 (now only a 0.073% change in  $\nu\Sigma_f$  in one fissile region causes a factor of 2 change in the eigenfunction).

In Table VI we present the estimates of the problem 3 eigenvalue during each of the ten 100-cycle spans

TABLE II

Estimates of  $k$  and its Standard Deviation for Problem 1

Cycles	Standard Monte Carlo	FMC Edge	FMC Average
1 to 100	0.997821 (0.008017)	0.999385 (0.000002)	0.999385 (0.000002)
101 to 200	0.999265 (0.005756)	0.999385 (0.000002)	0.999385 (0.000002)
201 to 300	0.998511 (0.006041)	0.999385 (0.000002)	0.999385 (0.000002)
301 to 400	0.998215 (0.005052)	0.999385 (0.000002)	0.999385 (0.000002)
201 to 500	0.999962 (0.004966)	0.999385 (0.000002)	0.999385 (0.000002)
501 to 600	0.999078 (0.005315)	0.999385 (0.000002)	0.999385 (0.000002)
601 to 700	0.999140 (0.005958)	0.999384 (0.000002)	0.999385 (0.000002)
701 to 800	0.999896 (0.006086)	0.999385 (0.000002)	0.999385 (0.000002)
801 to 900	0.999573 (0.006517)	0.999385 (0.000002)	0.999385 (0.000002)
901 to 1000	0.998926 (0.005389)	0.999385 (0.000002)	0.999385 (0.000002)

that we ran. As in problem 2, the FMC estimated standard deviations in  $k$  are about a factor of 7 smaller than the Monte Carlo estimates. (The accuracy of the FMC and Monte Carlo estimates of  $k$  is not so clear; this is discussed below.) As in problem 2, this happens even though the FMC eigenfunction estimates vary more from one cycle to the next than the Monte Carlo estimates. (But again, Fig. 8 shows that the FMC eigenfunctions averaged over 100 cycles are more accurate.)

Problems 2 and 3 show that for systems with fissile regions that are becoming weakly coupled, FMC esti-

mates of the eigenfunction can vary significantly from one cycle to the next, and this variation increases as the fissile regions increasingly decouple. This happens because (a) the eigenfunction in such physical systems becomes increasingly sensitive to small perturbations in the cross sections and (b) the number of Monte Carlo particles per cycle must be increased to avoid undersampling of the fission source. However, the eigenvalues in such systems are much less sensitive than the eigenfunctions, and indeed our FMC  $k$ -eigenvalue estimates for these problems are significantly more accurate than both the FMC eigenfunction estimates and the Monte Carlo eigenvalue estimates. We note that a factor of 6 difference in the FMC and Monte Carlo statistical errors in  $k$  (roughly seen in problems 2 and 3) translates into a factor of  $6^2 = 36$  computation time. That is, the Monte Carlo code would have to run about 36 times as many particles or cycles to obtain an accuracy comparable to the FMC results.

A close scrutiny of the above  $S_N$  and FMC results shows that there are small differences in their predicted values of  $k$ . Most notably, in problem 3 the fine-mesh  $S_{32}$  value of  $k$  is 0.9878, while the FMC-edge and FMC-average estimates are centered around 0.9880. These discrepancies are due to (a) small space-angle truncation errors in the  $S_N$  solution and (b) small systematic errors in the FMC solution caused by the fact that the functionals are evaluated using the Monte Carlo estimate of the flux, which has a systematically incorrect spatial shape (see Fig. 9). These various errors exist in all our  $S_N$  and FMC simulations, but they are most apparent in problem 3, which is the most difficult of the problems considered in this paper.

For eigenvalue problems with large absorbing regions, it may happen that very few or no Monte Carlo particles score in one or more spatial cells that are distant from a fission source. If no particles score, it is not possible to evaluate the functionals in Eqs. (14), since one would have to divide zero by zero. When this happens, or when the number of Monte Carlo particles that score in a cell is sufficiently small, we adopted the procedure of using the “diffusion” values of the functionals [given in Eqs. (17)] in the affected cells. Of course this is not desirable, but since it is done only in regions where  $\psi \approx 0$ , it has only a small impact on the eigenvalue and the eigenfunction estimates.

TABLE III

Data for Problem 2

Region	Location	$\Sigma_t$	$\Sigma_{s,0}$	$\Sigma_{s,n}$	$\nu \Sigma_f$
1	$0 < x < 5$	1.0	0.856	0.1	0.0
2	$5 < x < 10$	1.0	0.856	0.1	0.082
3	$10 < x < 17$	1.0	0.856	0.1	0.0
4	$17 < x < 22$	1.0	0.856	0.1	0.08235
5	$22 < x < 27$	1.0	0.856	0.1	0.0

IV. DISCUSSION

The Monte Carlo simulation of  $k$ -eigenvalue problems for optically thick fissile systems is made difficult by the statistical errors in the Monte Carlo process and the large dominance ratio of the system. When the fission source is undersampled, these effects yield estimates of the eigenfunction that wobble and fail to

FUNCTIONAL MONTE CARLO FOR  $k$ -EIGENVALUE

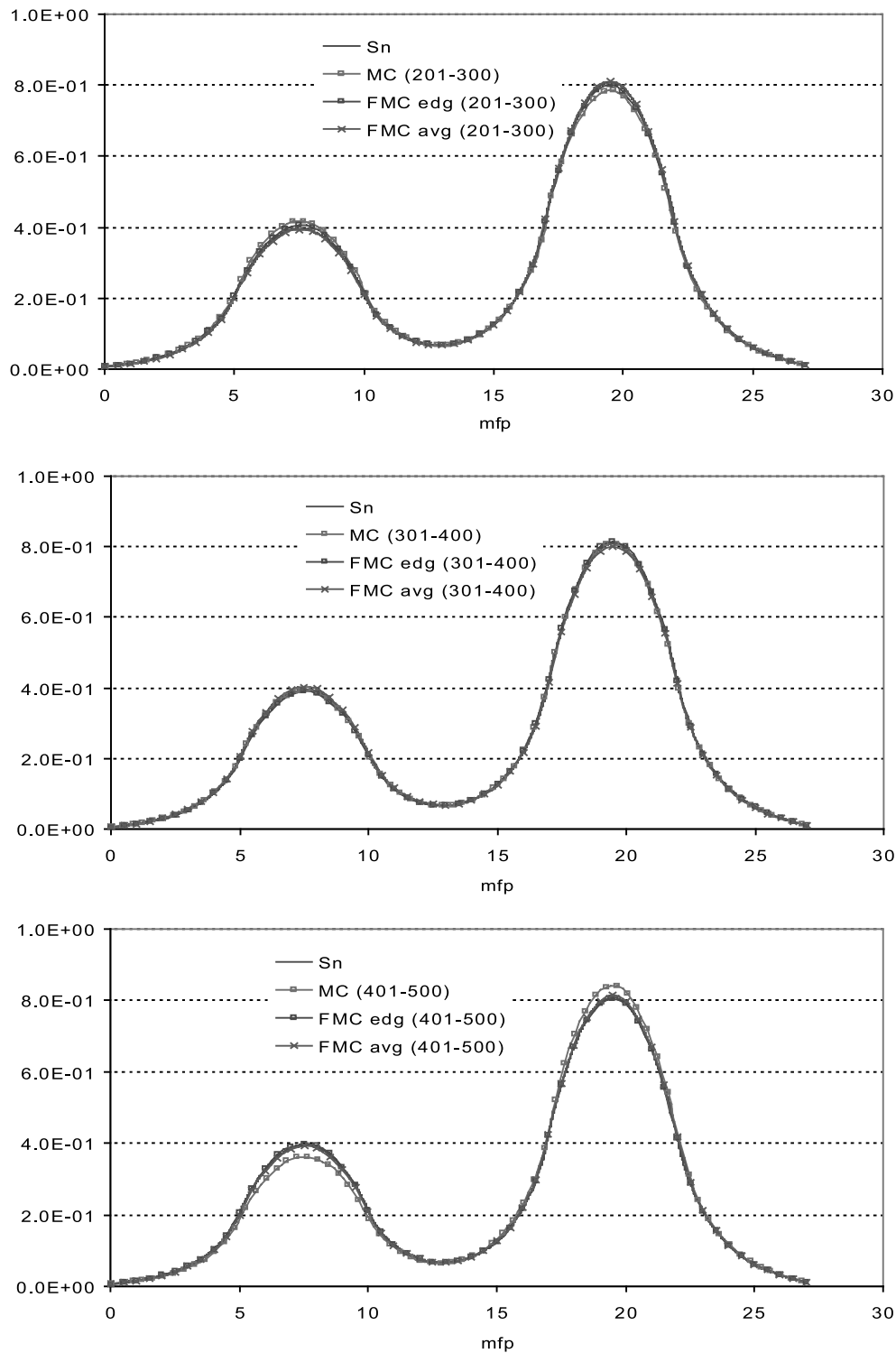


Fig. 6. Averaged problem 2 eigenfunction estimates during cycles 201 to 500.

converge, no matter how many inactive fission generations are performed. If the number of Monte Carlo particles per cycle is increased, the statistical errors decrease and the tilting can be controlled. However, for difficult

problems, sufficiently increasing the number of particles per cycle can be impractical.

In this paper we have outlined for a simple (planar geometry, monoenergetic)  $k$ -eigenvalue problem a new

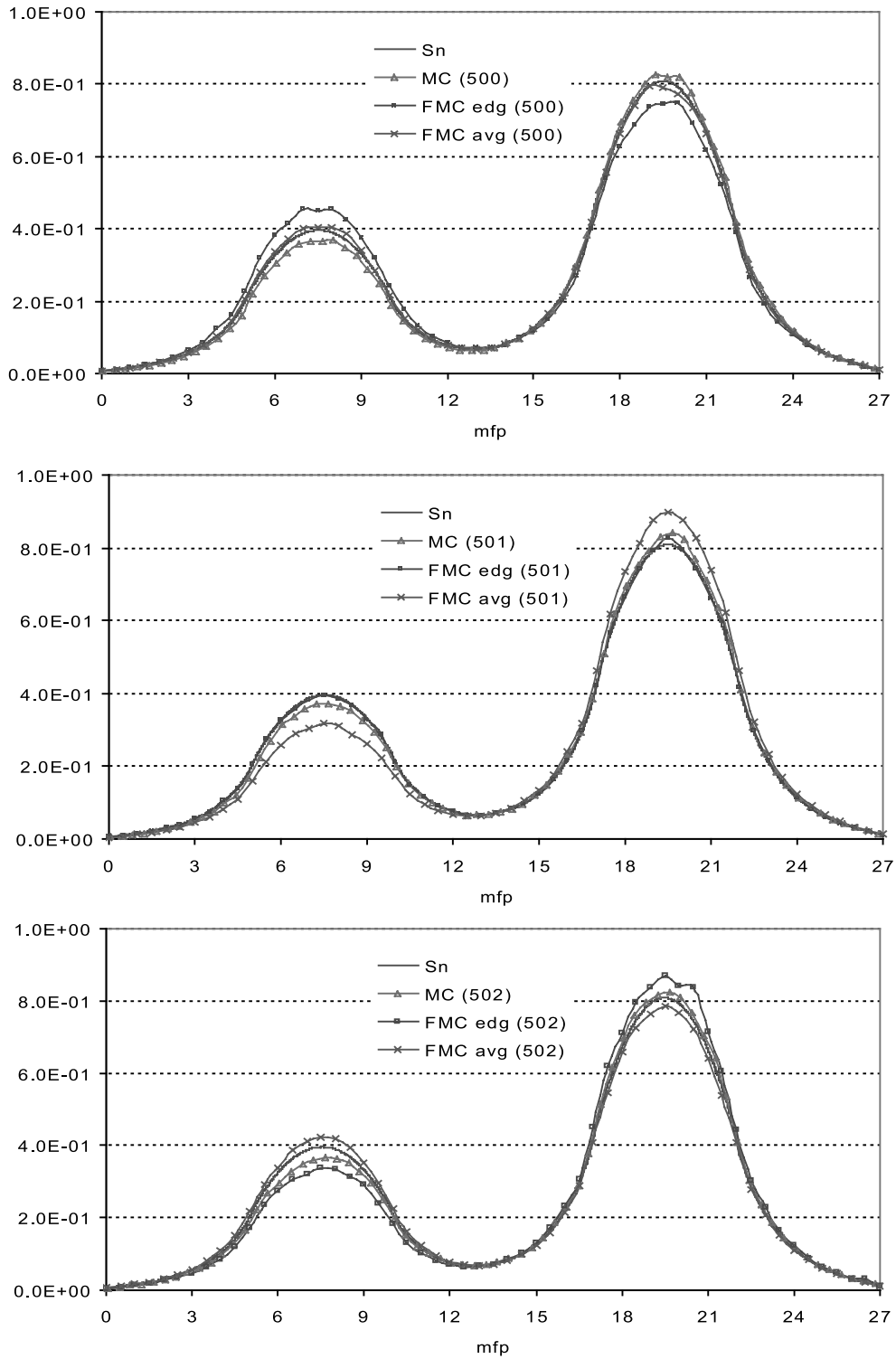


Fig. 7. Problem 2 eigenfunction estimates for cycles 500, 501, and 502.

functional Monte Carlo method that employs Monte Carlo only to estimate certain nonlinear functionals of the eigenfunction; these functionals are then used in a finite discrete system of low-order FMC equations to estimate

the eigenfunction and the eigenvalue. Because (a) the functionals are not sensitive to statistical errors in the eigenfunction estimates and (b) the low-order FMC equations are generally not sensitive to small statistical errors

TABLE IV

Estimates of *k* and its Standard Deviation for Problem 2

Cycles	Standard Monte Carlo	FMC Edge	FMC Average
1 to 100	0.986738 (0.049847)	0.992334 (0.001936)	0.992191 (0.002040)
101 to 200	0.992978 (0.004174)	0.992366 (0.000542)	0.992467 (0.000586)
201 to 300	0.992588 (0.004241)	0.992477 (0.000592)	0.992550 (0.000549)
301 to 400	0.992205 (0.003109)	0.992456 (0.000547)	0.992467 (0.000584)
401 to 500	0.993131 (0.004485)	0.992482 (0.000572)	0.992428 (0.000497)
501 to 600	0.992552 (0.003852)	0.992537 (0.000565)	0.992466 (0.000555)
601 to 700	0.992804 (0.003746)	0.992357 (0.000584)	0.992549 (0.000566)
701 to 800	0.992950 (0.004151)	0.992549 (0.000562)	0.992427 (0.000562)
801 to 900	0.992437 (0.003892)	0.992488 (0.000531)	0.992365 (0.000562)
901 to 1000	0.993166 (0.004379)	0.992471 (0.000535)	0.992508 (0.000521)

TABLE VI

Estimates of *k* and Its Standard Deviation for Problem 3

Cycles	Standard Monte Carlo	FMC Edge	FMC Average
1 to 100	0.982034 (0.055026)	0.987777 (0.002013)	0.987896 (0.001993)
101 to 200	0.988434 (0.004639)	0.988028 (0.000639)	0.987987 (0.000563)
201 to 300	0.988080 (0.004442)	0.987964 (0.000616)	0.988009 (0.000524)
301 to 400	0.987184 (0.003715)	0.987955 (0.000651)	0.987911 (0.000494)
401 to 500	0.988301 (0.004660)	0.987989 (0.000586)	0.987983 (0.000611)
501 to 600	0.987823 (0.003937)	0.988020 (0.000620)	0.987982 (0.000565)
601 to 700	0.987924 (0.003958)	0.987917 (0.000627)	0.987987 (0.000548)
701 to 800	0.988492 (0.004396)	0.988047 (0.000588)	0.988053 (0.000576)
801 to 900	0.987652 (0.004115)	0.988105 (0.000536)	0.988035 (0.000587)
901 to 1000	0.987753 (0.004481)	0.987958 (0.000549)	0.988137 (0.000572)

TABLE V

Data for Problem 3

Region	Location	$\Sigma_t$	$\Sigma_{s,0}$	$\Sigma_{s,n}$	$\nu\Sigma_f$
1	0 < <i>x</i> < 5	1.0	0.856	0.1	0
2	5 < <i>x</i> < 10	1.0	0.856	0.1	0.082
3	10 < <i>x</i> < 20	1.0	0.856	0.1	0
4	20 < <i>x</i> < 25	1.0	0.856	0.1	0.08206
5	25 < <i>x</i> < 30	1.0	0.856	0.1	0

in the functionals, the resulting FMC estimates of the eigenfunction and the eigenvalue are generally more accurate than standard Monte Carlo estimates.

In effect, the FMC method converts—with no approximation—the *k*-eigenvalue problem for the *continuous* transport problem [Eqs. (1)] into a low-order *matrix* eigenvalue problem [Eqs. (15)] in which the coefficients of the matrix (a) depend insensitively on the continuous eigenfunction and (b) are estimated by standard Monte Carlo methods. If the solution of the continuous *k*-eigenvalue problem is not sensitive to small perturbations in the cross sections in the system, the

solution of the low-order matrix equation should generally have statistical errors comparable to the small statistical errors in the matrix coefficients.

However, problems with weakly coupled fissile regions are inherently less stable, in the sense that small perturbations in the cross sections for these systems can yield large changes in the eigenfunction (but, fortunately, not the eigenvalue). The FMC method for such problems reflects these facts and yields eigenfunction estimates that vary significantly more from one cycle to the next than the eigenvalue estimates. In these situations, our simulations show that in spite of the relatively large cycle-to-cycle variations in the FMC eigenfunction estimates (compared to the cycle-to-cycle variations in the Monte Carlo eigenfunction estimates), the FMC eigenvalue estimates averaged over active cycles are significantly more accurate than the corresponding Monte Carlo eigenvalue estimates. It is possible that this is caused by a significantly smaller correlation in the FMC eigenfunction estimates from one cycle to the next compared to standard Monte Carlo. (This point is discussed again below.)

Also, although the FMC-average eigenfunction estimates are less noisy than the FMC-edge eigenfunction estimates, the FMC-average and FMC-edge eigenvalue

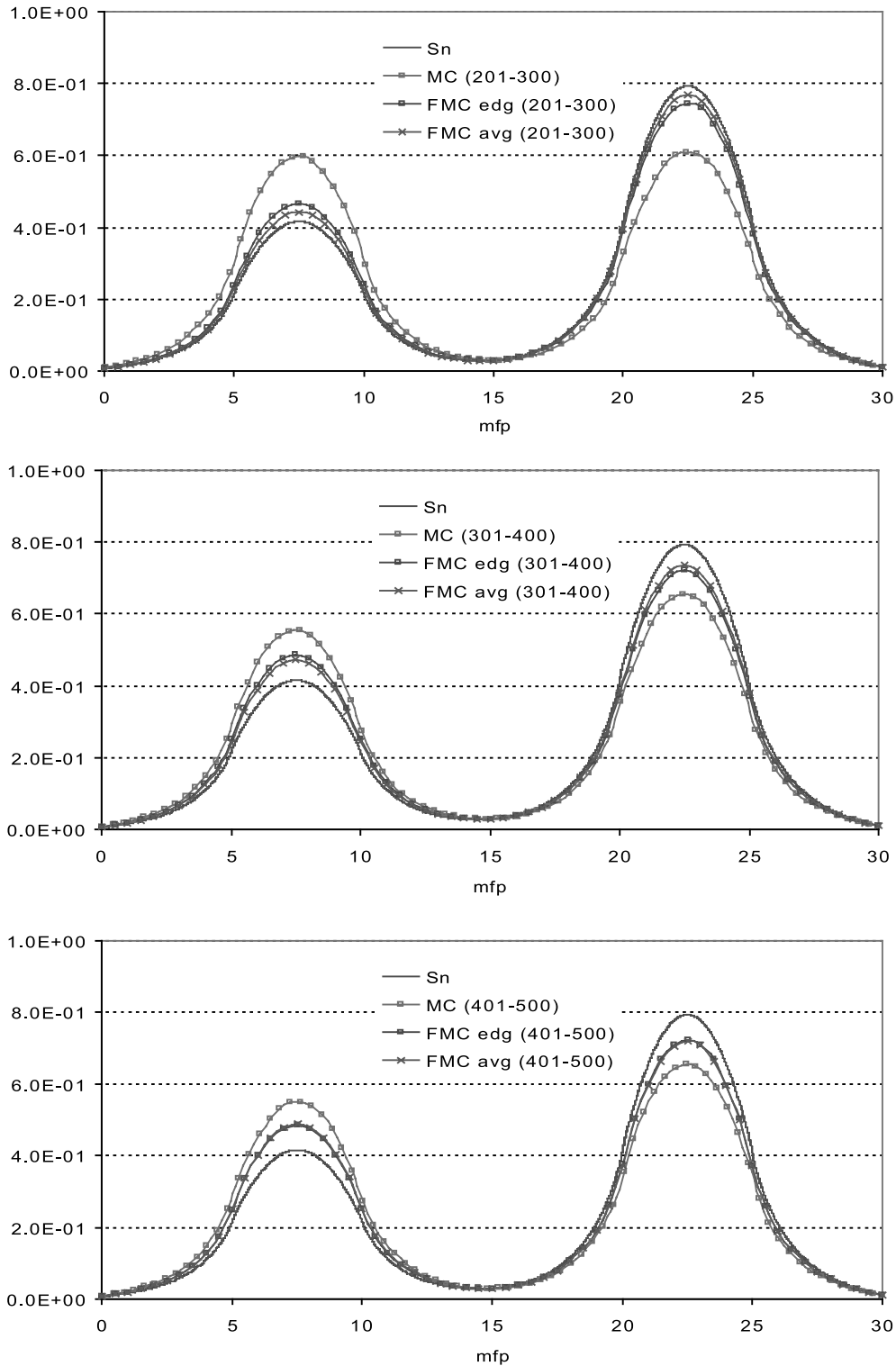


Fig. 8. Averaged problem 3 eigenfunction estimates during cycles 201 to 500.

estimates are of comparable high quality. At present, this good feature of the FMC method is not understood.

In this initial presentation of the FMC method, we have chosen the physical problem and the numerical pro-

cedures to be very simple. Thus, the physical problem discussed here is one-dimensional rather than three-dimensional, and monoenergetic rather than multigroup or continuous in energy. Also, the low-order FMC

FUNCTIONAL MONTE CARLO FOR  $k$ -EIGENVALUE

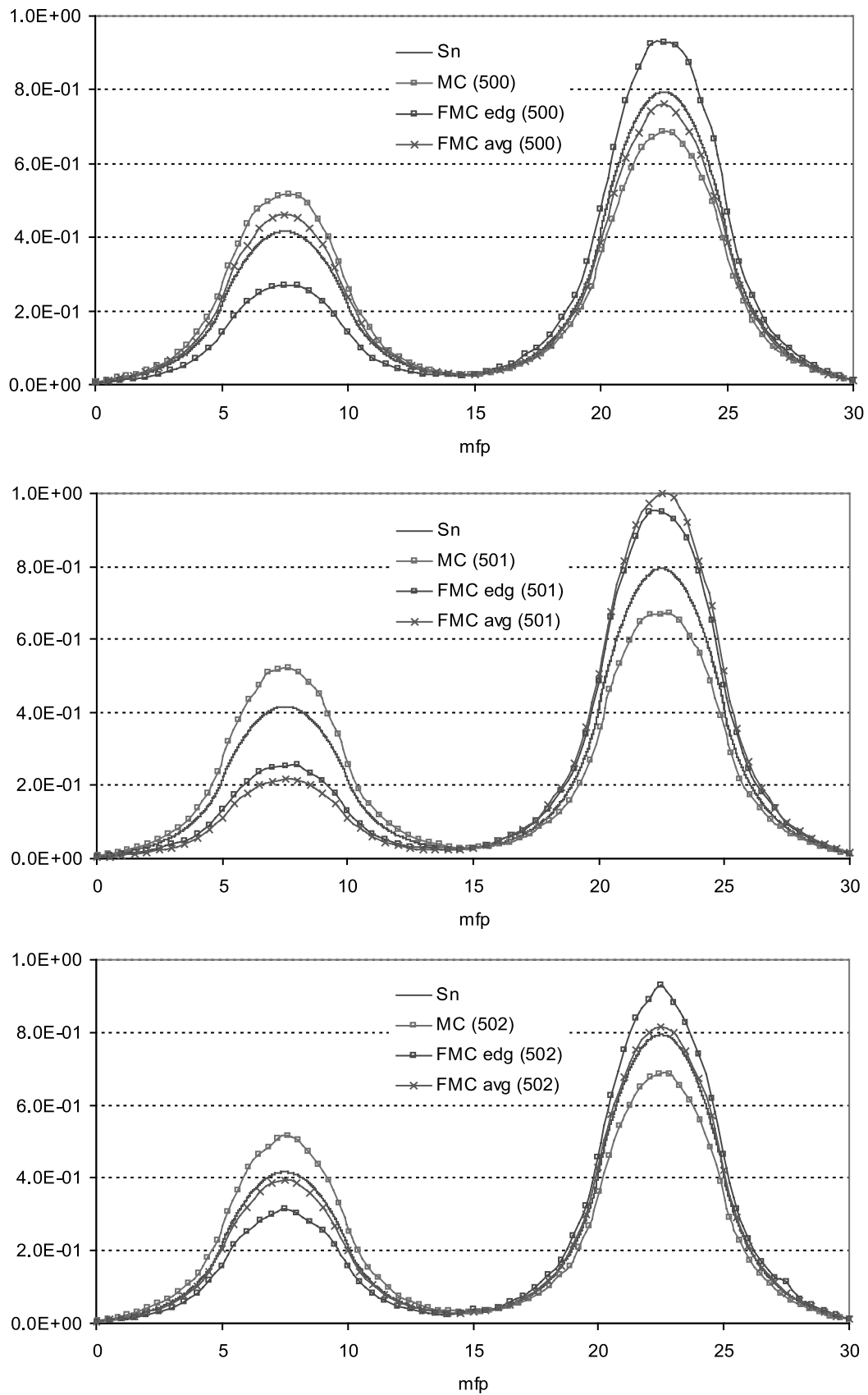


Fig. 9. Problem 3 eigenfunction estimates for cycles 500, 501, and 502.

simulations presented here were obtained as a post-processing that did not influence the high-order Monte Carlo simulations of Eqs. (1).

However, we have recently implemented the FMC method for one-dimensional multigroup problems, and we are confident that the method can be extended to three-dimensions. Also, in a more sophisticated FMC approach, it would be logical to use the FMC estimate of the eigenfunction to help construct the fission source for the next generation. Other issues, such as the efficiency of the FMC method as a function of the size of the spatial grid should also be examined. In addition, the estimated standard deviation in  $k$  for conventional Monte Carlo simulations is often much smaller than the true standard deviation, because of the correlations that exist in the fission source from cycle to cycle. The FMC method also certainly has cycle-to-cycle correlations in its eigenfunction and the eigenvalue estimates, and these *appear* to be smaller than in standard Monte Carlo. However, the magnitude of these FMC correlations and their effect is not presently known.

Finally, the FMC method is not restricted to eigenvalue problems; it can also be applied to fixed source problems in which global estimates of the flux are desired. If Monte Carlo estimates of the appropriate nonlinear functionals are generally more accurate than estimates of the flux itself, then this approach could be advantageous. However, the examination of all these ideas must be considered in future work.

#### ACKNOWLEDGMENT

We gratefully acknowledge support of this research through the U.S. Department of Energy NEER grant DE-FG07-04-ID14608.

#### REFERENCES

1. T. YAMAMOTO, T. NAKAMURA, and Y. MIYOSHI, "Fission Source Convergence of Monte Carlo Criticality Cal-

culations in Weakly Coupled Fissile Arrays," *J. Nucl. Sci. Technol.*, **37**, 41 (2000).

2. R. N. BLOMQUIST and E. M. GELBARD, "Alternative Implementations of the Monte Carlo Power Method," *Nucl. Sci. Eng.*, **141**, 85 (2002).

3. T. UEKI and F. B. BROWN, "Stationarity Modeling and Informatics-Based Diagnostics in Monte Carlo Criticality Calculations," *Nucl. Sci. Eng.*, **149**, 38 (2005).

4. T. UEKI, "Information Theory and Undersampling Diagnostics for Monte Carlo Simulation of Nuclear Criticality," *Nucl. Sci. Eng.*, **151**, 283 (2005).

5. R. N. BLOMQUIST, M. ARMISHAW, D. HANLON, N. SMITH, Y. NAITO, J. YANG, Y. MIOSHI, T. YAMAMOTO, O. JACQUET, and J. MISS, "Source Convergence in Criticality Safety Analyses," NEA Report No. 5431, Nuclear Energy Agency, Organisation for Economic Co-operation and Development; Available on the Internet at [www.nea.fr/html/science/pubs/2006](http://www.nea.fr/html/science/pubs/2006) (Nov. 2006).

6. T. UEKI, "On-the-Fly Diagnostics of Particle Population in Iterated-Source Monte Carlo Methods," *Nucl. Sci. Eng.*, **158**, 15 (2008).

7. V. YA. GOL'DIN, "A Quasi-Diffusion Method for Solving the Kinetic Equation," *ZH. Vych. Mat.*, **4**, 1078 (1964); English translation published in *USSR Comput. Math. and Math. Phys.*, **4**, 6, 136 (1967).

8. D. Y. ANISTRATOV and V. YA. GOL'DIN, "Nonlinear Methods for Solving Particle Transport Problems," *Transport Theory Stat. Phys.*, **22**, 42 (1993).

9. D. Y. ANISTRATOV, "Consistent Spatial Approximation of the Low-Order Quasidiffusion Equations on Coarse Grids," *Nucl. Sci. Eng.*, **149**, 138 (2005).

10. M. L. ADAMS and E. W. LARSEN, "Fast Iterative Methods for Discrete-Ordinates Particle Transport Calculations," *Prog. Nucl. Energy*, **40**, 3 (2002).

11. M. A. COOPER and E. W. LARSEN, "Automated Weight Windows for Global Monte Carlo Deep Penetration Neutron Transport Calculations," *Nucl. Sci. Eng.*, **137**, 1 (2001).